Gulf of Mexico Gas Hydrate Joint Industry Project Leg II:
Alaminos Canyon 21 Site Summary

Matthew Frye[1], William Shedd[2], Paul Godfriaux[2], Timothy Collett[3], Myung Lee[3], Ray Boswell[4], Rebecca Dufrene[2], & Dan McConnell[5]

Abstract

The primary goal of the Gulf of Mexico Joint Industry Project (JIP) Leg II drilling program was to locate and record the occurrence of gas hydrate in high-quality deepwater sand reservoirs. In the first week of May 2009, the JIP utilized the Helix *Q-4000* semi-submersible to drill and log two wells in the Diana sub-basin in the northwestern Gulf of Mexico at the Alaminos Canyon (AC) 21 site. The AC 21-A and AC 21-B wells confirmed the presence of an areally extensive, sand-rich deepwater fan system that was predicted from industry 3-D seismic data and existing industry well penetrations. The primary targets were encountered within 600 ft of the seafloor, well above the predicted base of gas hydrate stability depth of approximately 1,500 feet below sea floor (fbsf). The target sand reservoirs as seen in the A and B wells measured 62 ft and 125 ft, respectively, and contained elevated formation resistivity consistent with low to moderate saturations of gas hydrate (20% to 40%). The interface between the overlying shales and the hydrate-bearing sands is one of high acoustic impedance, thus providing an anomalous response on the 3-D seismic data with a strong peak-leading top.

Introduction

In April and May 2009, the Gulf of Mexico (Gulf of Mexico) Gas Hydrate Joint Industry Project (the "JIP") conducted its Leg II operations at three sites in the northern Gulf of Mexico (Figure F1) using the semi-submersible Helix *Q-4000* (Boswell *et al*., 2009a). These locations were selected to test geological and geophysical analyses conducted with the intent of locating gas hydrate-bearing sand reservoirs (Hutchinson *et al*., 2009a, 2009b; Shedd *et al*., 2009b) and conducting comprehensive logging while drilling (LWD) operations (Collett *et al*., 2009b) in advance of planned Leg III coring and pressure coring. This report presents the geologic setting and initial scientific results of LWD operations conducted at the Alaminos Canyon block 21 site (Site AC 21). Detailed descriptions of the LWD operations and data acquisition for this site are provided in Mrozewski *et al*. (2009) and Guerin *et al*. (2009).

The AC 21 site lies within the northwestern Gulf of Mexico along the boundary between the Alaminos Canyon and East Breaks (EB) protraction areas (Figure F2). It is one of two drill sites evaluated by the JIP for possible Leg II operations within the Diana intra-slope basin (Shedd *et al*., 2009b). Three well locations were permitted at Site AC 21 to test gas hydrate targets, including two wells in block AC 21 and a third in block AC 65. An additional drill site, including four permitted wells, was in East Breaks (EB) block 992 (Site EB 992). Both sites featured very similar geologic targets. Site EB 992 is approximately nine miles to the east/northeast of Site AC 21 and located in the central part of the Diana basin (Figure F2). At all of the target locations, thick sandstone reservoirs (50 ft to 200 ft) were predicted based on the integration of existing industry well data and seismic attribute analysis from 3-D seismic data. Low to moderate saturations of gas hydrate were predicted

[1]Minerals Management Service
381 Elden St.
Herndon, VA 20170
E-mail:
matt.frye@mms.gov

[2]Minerals Management Service
1201 Elmwood Park Blvd.
New Orleans, LA 70123-2394
E-mail:
Dufrene: rebecca.dufrene@mms.gov
Godfriaux: paul.godfriaux@mms.gov
Shedd: william.shedd@mms.gov

[3]US Geological Survey
Denver Federal Center, MS-939
Box 25046
Denver, CO 80225
E-mail:
Collett: tcollett@usgs.gov
Lee: mlee@usgs.gov

[4]National Energy Technology Laboratory
U.S. Department of Energy
P.O. Box 880
Morgantown, WV 26507
E-mail:
ray.boswell@netl.doe.gov

[5]AOA Geophysics Inc.
2500 Tanglewilde Street
Houston, TX 77063
E-mail:
dan_mcconnell@aoageophysics.com

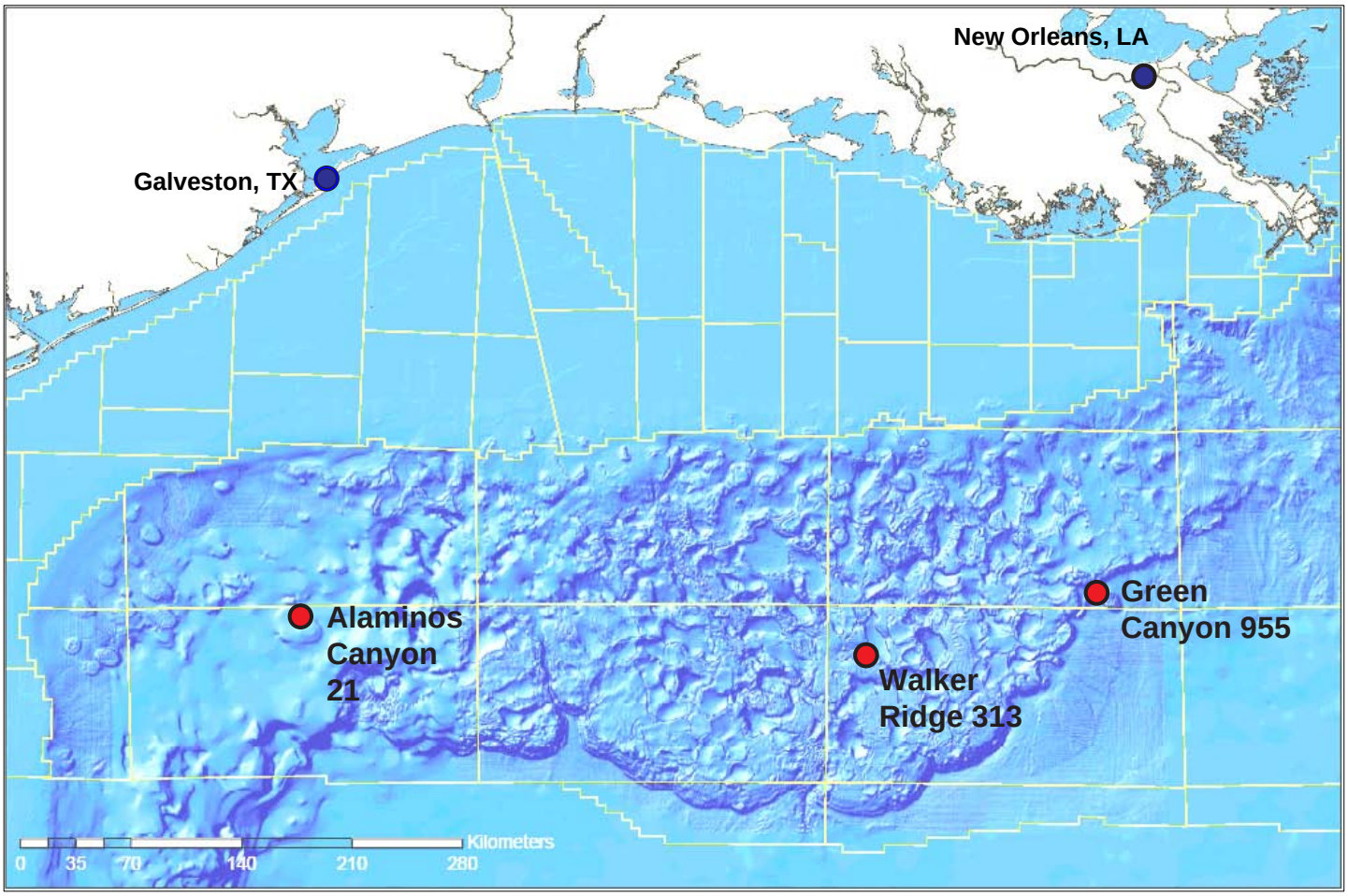

Figure F1: *Northern Gulf of Mexico showing location of the three JIP sites visited during Leg II.*

in these reservoirs based on the slightly elevated formation resistivity measured in the EB 992 #001 industry well and the high impedance leading peak event associated with the seismically-defined top of the sandy facies. A primary scientific objective of the drilling was to collect high-quality LWD data through this sand facies to further refine estimates of gas hydrate saturations.

The Diana basin is located in the northwestern Gulf of Mexico, approximately 160 miles south of Galveston, TX (Figure F1). Water depth in the basin center averages 4800 ft (Figure F2). The basin is bounded by relatively shallow salt bodies and contains mostly Pliocene- and Pleistocene-age sand sequences bounded by marine shales. Existing well log and core data from industry wells in the Diana basin confirm the occurrence of thick sand sequences within the shallow section. Depositional environment throughout the Tertiary section is interpreted to consist of deepwater turbidites and mass transport complexes.

The Diana basin contains five producing oil and gas fields in the EB and AC protraction areas, including Diana (EB 945), South Diana (AC 65), Marshall (EB 949), Madison (AC 24), and Hoover (AC 25) (Figure F2). The Rockefeller field in EB 992 is currently under development by the operator. All of the fields are processed through the Hoover production spar facility in AC 25, which commenced production in 2000. Cumulative production from the fields as of April, 2009, has exceeded 90 million barrels of oil and 465 billion cubic ft (BCF) of gas. Completion depths are typically 5000 to 8000 fbsf in Lower Pleistocene and Upper Pliocene reservoirs (Sullivan and Templet, 2002; Symington and Higgins, 2000). Previous geologic interpretations of these reservoir systems reveal a complex distribution of sand-rich deepwater facies that includes confined feeder channel systems, weakly confined/distributary channel complexes, and distributary lobe and sheet complexes (Sullivan and Templet, 2002; Sullivan *et al*., 2004).

The 3-D seismic data in the Diana basin reveals (in places) a possible bottom simulating reflector (BSR) that is

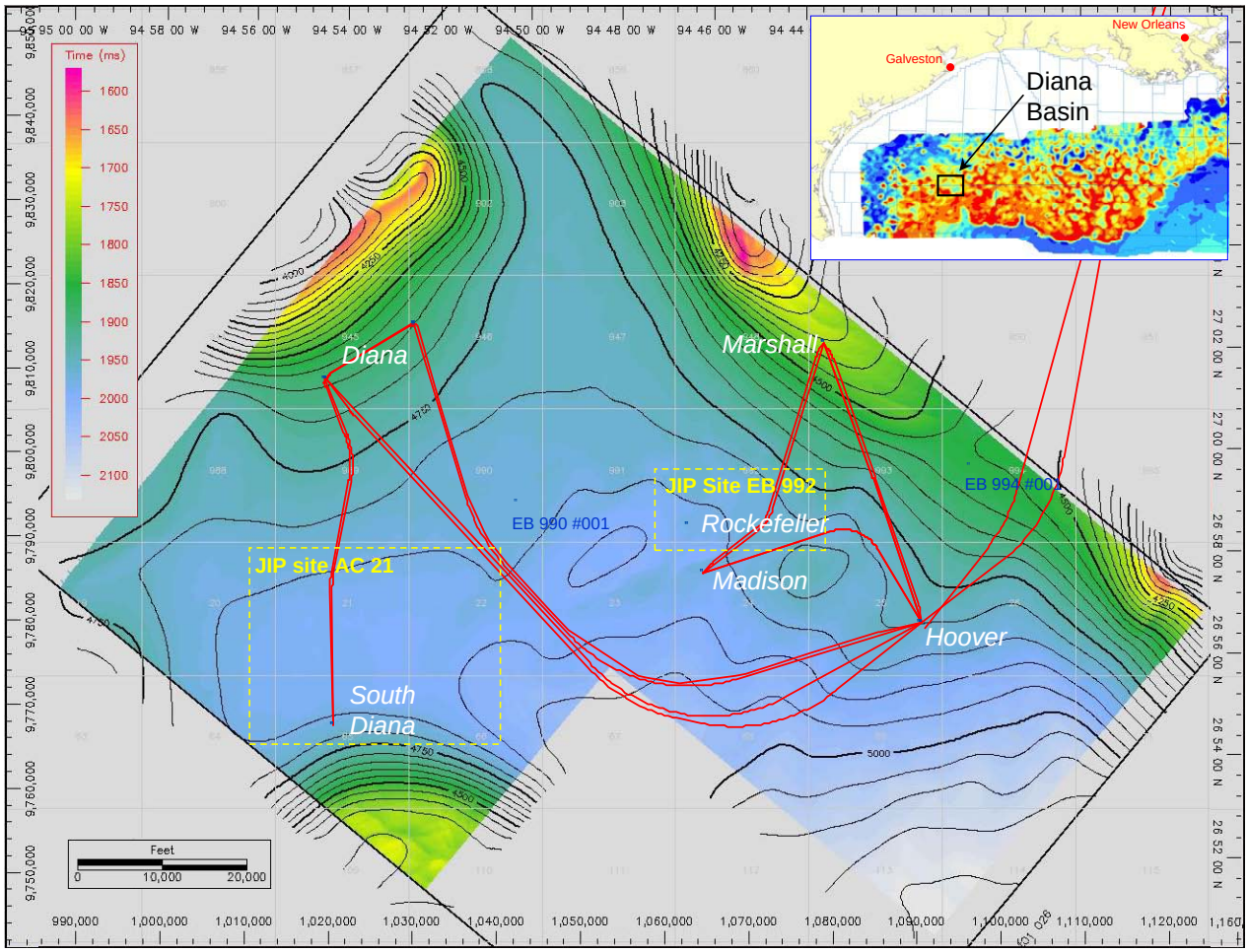

Figure F2: *Location map for the Diana basin in the western Gulf of Mexico. Water Depth for the basin shown as two way travel time (color grid) and feet (contours). JIP sites AC 21 and EB 992 are outlined by yellow dashed polygons. Surface locations of industry wells are shown as blue squares; oil and gas fields are labeled in white. Pipelines from producing fields are shown in red. Underlying seismic data courtesy of WesternGeco.*

interpreted to represent the base of gas hydrate stability (Figure F3). Previous authors have also noted this feature (Dai *et al*., 2004; Shedd *et al*., 2009b). The depth of this reflector varies across the basin, but typically remains within a window that is between 1000 and 1500 fbsf. In general, the BSR is recognized in a deeper position in the center of the basin and shallower near the basin margins. It is worth noting that the occurrence of a BSR on seismic data may not have any substantive relation to the occurrence of gas hydrate in the target sand reservoirs. Conversely, the absense of a BSR does not necessarily indicate the absence of gas hydrate in the system.

In the first part of this report, pre-drill data and interpretations are presented to support the exploratory analysis that guided target selection at Sites AC 21 and EB 992. The second part of the report includes detailed LWD results from Site AC 21 and an integrated analysis of the petroleum system that incorporates these results.

Pre-Drill Site Evaluation and Target Selection

Data Availability

The Gulf of Mexico JIP Leg II well locations in the Diana basin were selected after a careful integration of available data, including existing industry well logs, paleontological reports, checkshot velocity surveys, and 3-D seismic data.

Industry Wells

Largely due to the maturity of the Diana basin as a producing oil and gas province, nearly all of the industry well logs in the area are available as public information (surface locations shown in Figure F2). Table T1 is a listing of the key wells in the basin included in our analysis.

Figure F3: *Arbitrary seismic section showing a BSR in the Diana basin. Length of section approximately 20 miles (32 km). Vertical scale in two-way time. Seismic data courtesy of WesternGeco.*

All of the shallow logs used in the pre-drill interpretation of possible gas hydrate occurrence are LWD data acquired in open holes ranging from 24 to 30 inches in diameter. These large open holes do not provide optimum measurement conditions for the logging tools, and the acquired log values and subsequent interpretations of lithology, fluid saturation, and other parameters were evaluated considering these limitations. Additionally, critical data including porosity, formation density, and acoustic measurements were not acquired in the potentially hydrate-bearing shallower section of the industry wells.

The EB 992 #001 well was evaluated prior to the Leg II drilling program and interpreted to contain gas hydrate throughout a sand interval 135 ft-thick (Figure F4A). The top of the hydrate-bearing sand is 767 fbsf (5,720 ft driller's depth). The gamma ray log character is blocky and contains a sharp base and a sharp top, with a minimal amount of intervening shale. Estimated gas hydrate saturations, calculated using the quick-look method presented by Collett (1998, 2000), are approximately 30% for this interval (Figure F4B). Resistivity in the interpreted hydrate-bearing interval or section measures between 1.5 and 2 ohm meters (Ω-m).

The EB 994 #001 well contains a shallow sand interval that exceeds 450 ft thick, with the top of the sand located at a depth of 389 fbsf and the base at 844 fbsf. The entire sand interval is interpreted to be water-saturated (not hydrate-bearing). The well is important, however, in that the low clay content sands (based on the tracking of low gamma ray response and low formation resistivity) provide high-confidence background resistivity (R_o) values (as low as 0.2 Ω-m) necessary for the quick-look saturation method used on the EB 992 #001 well. The gamma ray log character of the shallow sand in the EB 994 #001 indicates a sharp base and a gradational top. Similar to EB 992 #001 well, the blocky sand interval in the EB 994 #001 spans the lower 175 ft with minimal interbedded shales. The upper 275 ft can be subdivided into four sequences with fining-up grain sizes and varying clay content, measuring from 30 to 80 ft thick, separated by shale intervals in the 10 to 20 ft range.

Area	Block (bhl)	Lease	Well No.	API	WD (ft)	KB (ft)	Log Top (ft)	Log Bottom (ft)	Log Date	Operator	Longitude (surface)	Latitude (surface)
EB	945	G08211	#002	608044016200	4653	86	4984	11309	1996_Jan_13	Exxon Exploration	-94.875583	27.034778
EB	946	G08212	#003	608044018100	4653	48	4946	10546	1998_Sept_19	Exxon Upstream	-94.875411	27.034758
EB	949	G10949	#001	608044017600	4356	48	4674	11107	1998_Jul_08	Exxon Company USA	-94.724617	27.027453
EB	990	G23255	#001	606044023300	4825	83	5150	14955	2002_June_08	ExxonMobil	-94.837964	26.977644
EB	992	G10325	#001	608044016000	4867	86	5196	12449	1995_Oct_24	Exxon Exploration	-94.774639	26.970556
EB	994	G12629	#001	608044016500	4645	86	4902	12475	1997_May_01	BP Exploration	-94.67057	26.98945
AC	24	G19379	#001	608054000500	4856	48	5153	13450	1998_May_30	Exxon Exploration	-94.769322	26.954831
AC	65	G09249	#001	608054000300	4852	86	5184	17000	1997_Feb_14	Exxon Exploration	-94.905584	26.905945

Table T1: *Industry wells in the vicinity of proposed JIP Leg II Sites AC 21 and EB 992.*

A

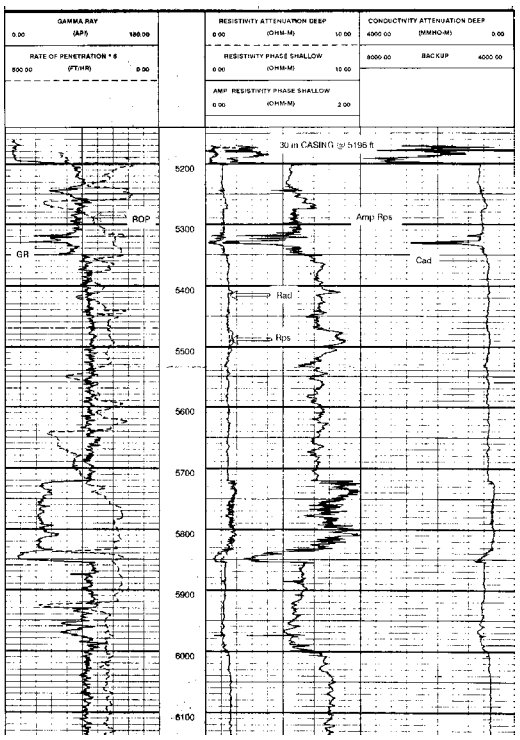

B

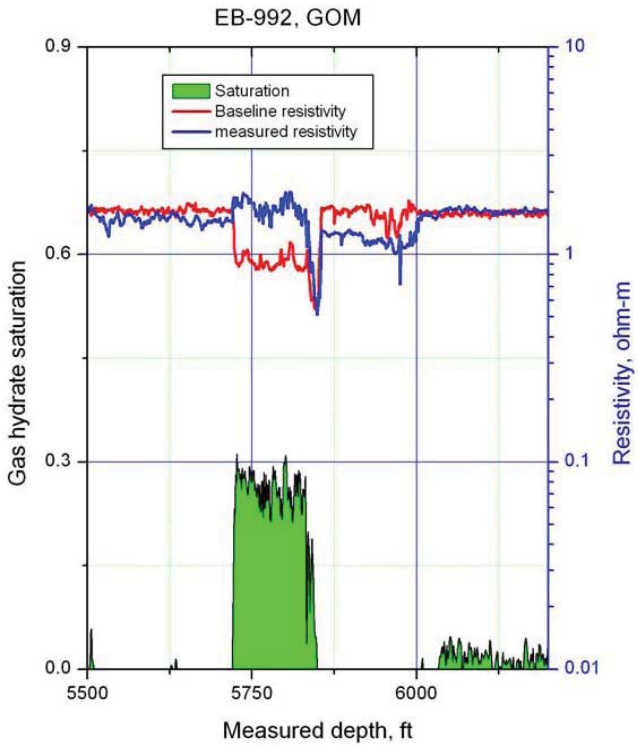

Figure F4: *(A) EB 992 #001 well log image (B) Gas hydrate saturations estimated from the resistivity log in the EB 992 #001 well, using the quick-look method by Collett (2000).*

The EB 990 #001 well also contains a thick interval of water-saturated sand very high in the stratigraphic section. The top of the sand was not in the logged interval, which begins at 242 fbsf (36-inch surface casing jetted in above this depth). The base of the sand is at a depth 792 fbsf, for a total logged thickness that spans an interval of at least 550 ft. The sand has a sharp base as identified on the gamma ray, and at least seven unique intervals that, from the bottom, include: 70 ft fining-upward sequence, 160 ft blocky sand, 80 ft blocky sand, 40 ft fining-upward sequence, 50 ft fining-upward sequence, 60 ft fining-upward sequence, and a blocky sand at least 150 ft thick. Formation resistivity in the cleanest sand measures less than 0.2 Ω-m. The thickest shale break between the sand units is 10 ft.

Industry wells in AC 24, EB 945, EB 946, and EB 949 all contain variable amounts of thin sands (~10 ft thick) in the shallow section that are interpreted to be water-bearing. Additionally, an industry well in AC 65 records a sand with slightly elevated resistivity that will require additional study. These wells are considered valuable data points for the seismic stratigraphic analysis and seismic calibration described later in this report.

Biostratigraphy

In the deepwater Gulf of Mexico, calcareous nannofossils are collected to provide subsurface biostratigraphic zonation and to aid in horizon age identification. The industry nannofossil reports compiled for wells in the Diana basin generally start at depths far beneath the presumed base of gas hydrate stability, yielding information that is useful but not definitive for our target sands. However, two of the wells (EB 992 and EB 946) sampled *Pseudoemiliania lacunosa "A"* within 900 vertical feet beneath the seismically-inferred base of gas hydrate stability. On the MMS biostratigraphic chart (Witrock *et al*., 2003), this zonation would be roughly equivalent to the top of the Middle Pleistocene. The last appearance datum of *Pseudoemiliania lacunosa "A"* has been age dated at 0.44 million years (*my*) old (Gradstein *et al*., 2004). As the Diana basin gas hydrate targets are stratigraphically above this datum, we would expect them to be younger than 0.44 *my* old, and most likely of Upper Pleistocene age.

Check Shot Velocity Data

Downhole check shot velocity data are available from four wells in the study area (EB 990, EB 992, EB 946, and EB 994). These data allow for a non-synthetic well tie to seismic using time vs. depth relationships acquired from various depths in the wellbore. Unfortunately, no internal velocity data were acquired in the potential gas hydrate-bearing sand reservoir in the EB 992 #001 well.

Seismic Data

Most seismic data interpretation was performed on the *East Breaks/Alaminos Canyon 8-Q* multiclient 3-D Kirchhoff prestack time migration survey, acquired and licensed by Western Geco. Acquisition and processing parameters of the survey, which covers a contiguous area of approximately 250 square miles, are shown in Table T2. The dominant frequency (~50 hz) is nearly twice that found in most industry seismic data, and the final processed sample rate of the seismic volume is 2 milliseconds. Both of these parameters contribute to the excellent quality of the Western Geco *8-Q* data.

Integrated Geologic Analysis of the Potential Drill Sites

The pre-drill evaluation of the AC21 site integrated the available geologic and geophysical data in an effort to determine the drill locations with the greatest potential for encountering gas hydrate-bearing sand facies. This analysis of the total "gas hydrate petroleum system" (Boswell *et al*., 2005; Collett *et al*., 2009a) considers each of the key factors that contribute to the formation of gas hydrate occurrences, including (1) gas hydrate pressure-temperature-geochemical stability conditions, (2) the presence of a suitable host sediment or "reservoir", and (3) gas source and migration efficiencies.

Gas Hydrate Stability Conditions

Gas hydrate stability zone thickness across the Gulf of Mexico has been modeled in a number of studies (e.g. Milkov and Sassen, 2001; Marcucci and Forrest, 2007; Frye, 2008) that show pressure and temperature conditions are typically favorable where water depths that exceed 1000 ft. Locally in the Diana basin, where water depth averages 4800 ft in the basin center (Figure F2), the base of gas hydrate stability is modeled to occur ~1500 fbsf assuming ambient conditions of salinity (35 ppt), water bottom temperature (4° C), and geothermal gradient (~25° C/km). On the basin margins, where local salt is thought to increase both salinity (Bruno and Hanor, 2003; Hanor 2004, 2007) and heat flow (O'Brien and Lerche, 1988) in the shallow

Acquisition Parameters		Processing Parameters
Recording Vessel	Pride	Group forming
Recording System	Q-Marine*	Navigation merge
Line Orientation	NW/SE	Designature
Energy Source	Dual airgun arrays; 5085 in.3	Gain correction
Source Separation	50 m	Noise attenuation
Source Depth	5 m	Receiver motion correction
Shot Interval	25 m; 50 m per source; flip-flop	Demultiple
Streamer Length	8000 m	Water velocity correction
Streamer Depth	6 m	Inverse Q
Streamer Separation	100 m	Velocity analysis (1 km grid)
DGF Group Interval	12.5 m	Kirchhoff prestack time migration (0.5 km grid)
Record Length	10 sec	Velocity analysis (0.5 km grid)
Sample Rate	2 msec	Stack
# of DGF Channels	640 per streamer	RNA, filter and scale
Nominal Fold	80	Final cell size: 6.25 x 12.5 m
Final Bin Size	6.25x12.5 m; (parallel interleaved)	Final fold: 40
Survey Completed	2002	Final record length: 8.5 sec
		Final sample rate: 2 msec

Table T2: *Western Geco 8-Q survey parameters (Western Geco, 2009).*

section, the thickness of the stability zone may be reduced significantly. Figure F5 shows the predicted mean thickness of gas hydrate stability in the Diana basin using the spatial model and methodology described by Frye (2008).

The thermal regime in the Diana basin is estimated using the custom statistical thermodynamic prediction program *MMSHyd* by assuming that the bottom simulating reflector represents the depth of gas hydrate stability (e.g. Yamano *et al*., 1982; Harris *et al*., 2007). Calculated geothermal gradients (based on seismic depth to BSR, 4° C water bottom temperature, 35 ppt salinity, and 100% methane) range from approximately 20° C/km to 30° C/km across the basin. Equilibrated bottom hole temperature measurements from producing reservoirs in the area are used to verify these calculations.

Reservoir Conditions

A key objective of JIP Leg II was the evaluation of sand-rich reservoir facies within the gas hydrate stability zone. Figure F6 is an arbitrary seismic section through the EB 992 #001 well location, where the shallow stratigraphy is representative of that present across the AC 21 and EB 992 JIP sites. The stratigraphic section is divided into five informal units based on the seismic character and corresponding well log response in the EB 992 #001. Unit 1, which begins at the mudline, is ~250 ft thick and appears as parallel, continuous reflectors on the seismic section. This interval is not logged in the EB 992 #001, but is interpreted to comprise shales deposited as a hemipelagic drape in the absence of any significant coarse-grained clastic input into the basin. Unit 2 is ~500 ft thick at the well location where it appears seismically as a low-frequency, un-bedded homogeneous unit. Unit 2 is predominantly shale in the #001 well with a thin sandy interval near the top. This unit is interpreted to be part of a sand-poor mass transport complex. Unit 3 is a 135 ft-thick sand package with a strong seismic peak marking the top, and a strong seismic trough marking the base (Figure F7). No consistent internal seismic reflections are noted. This sand unit is interpreted to comprise a complex lowstand deepwater fan assemblage that represents the primary JIP gas hydrate target in the Diana basin. The predicted lithofacies character and distribution of Unit 3 is described in much greater detail in the following section. Unit 4 is a relatively thin (~150 ft) interval of shale and interbedded silt/sand that generates a regionally-extensive unit of continuous, parallel seismic reflectors. The strong seismic peak at the base of Unit 4 corresponds to an abrupt increase in formation resistivity that is recognized in nearly every well in the Diana basin. This peak seismic event is referred to hereafter as “Regional 1” as it can be tracked across the entire basin (Figure F8). The Regional 1 horizon is also used in the analysis of seismic attribute data described later in the report. Unit 5 is a shale-dominated interval below the Regional 1 horizon that is characterized seismically by a chaotic zone of mostly

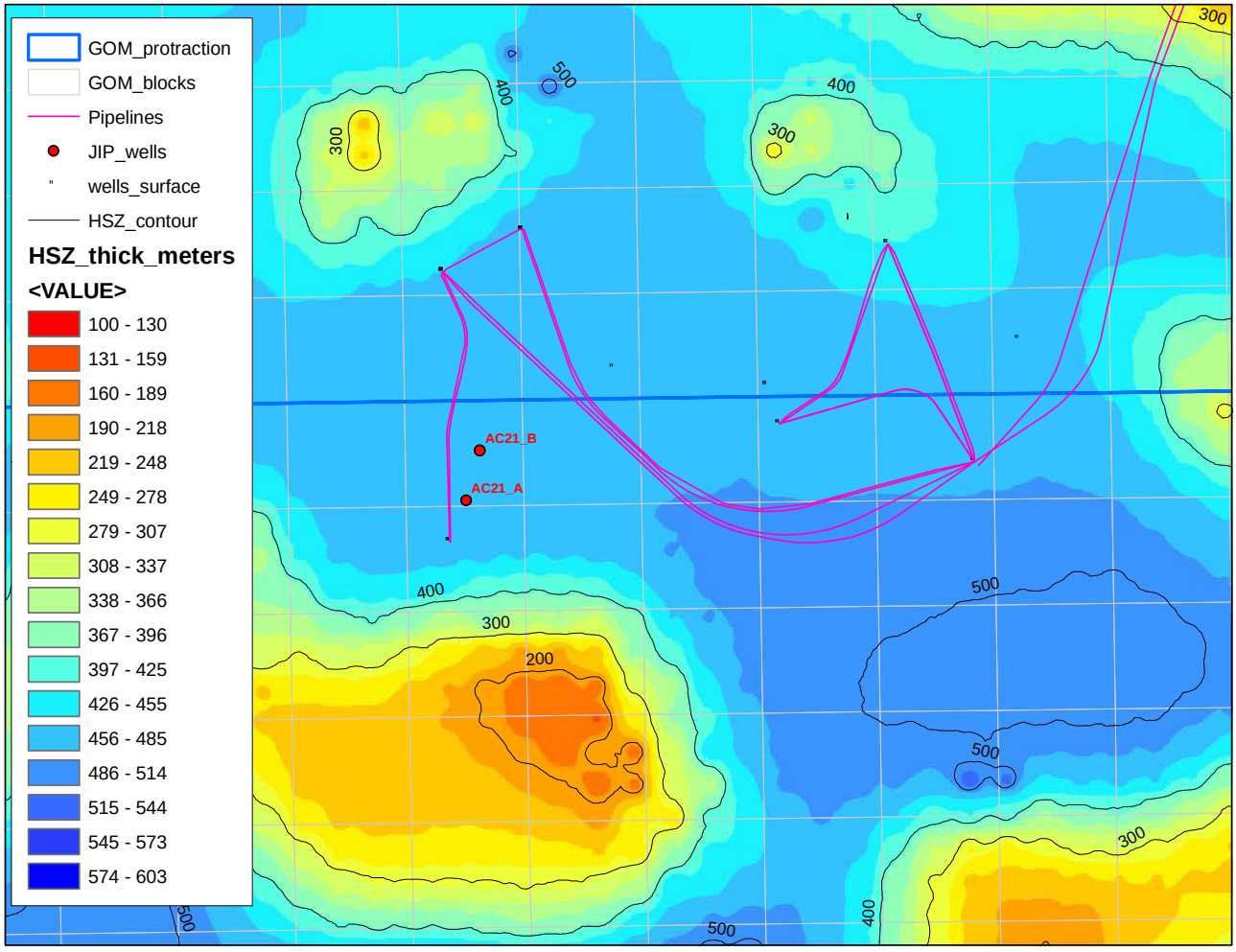

Figure F5: *Gas hydrate stability zone (HSZ) thickness calculated using spatial model and methodology presented by Frye (2008). Thickness reported in meters.*

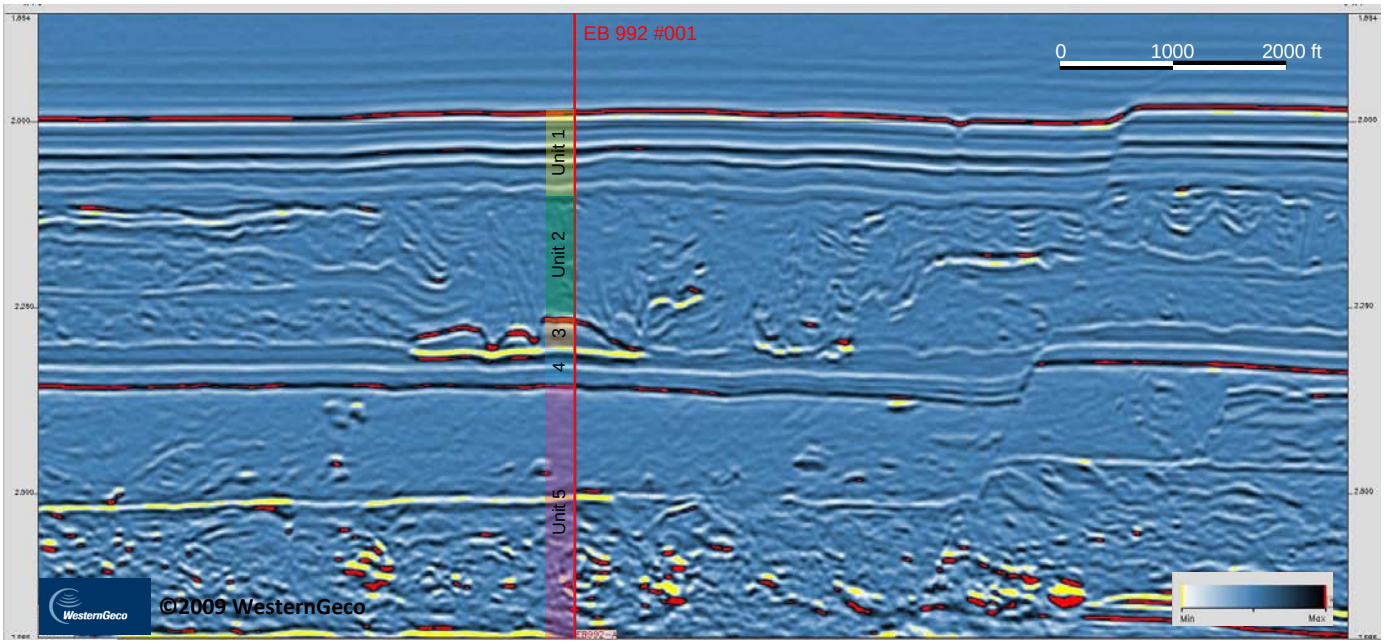

Figure F6: *Arbitrary seismic section though EB 992 #001 well, showing five informal stratigraphic units. Vertical axis is two-way travel time. See text for description of units. Seismic data courtesy of WesternGeco.*

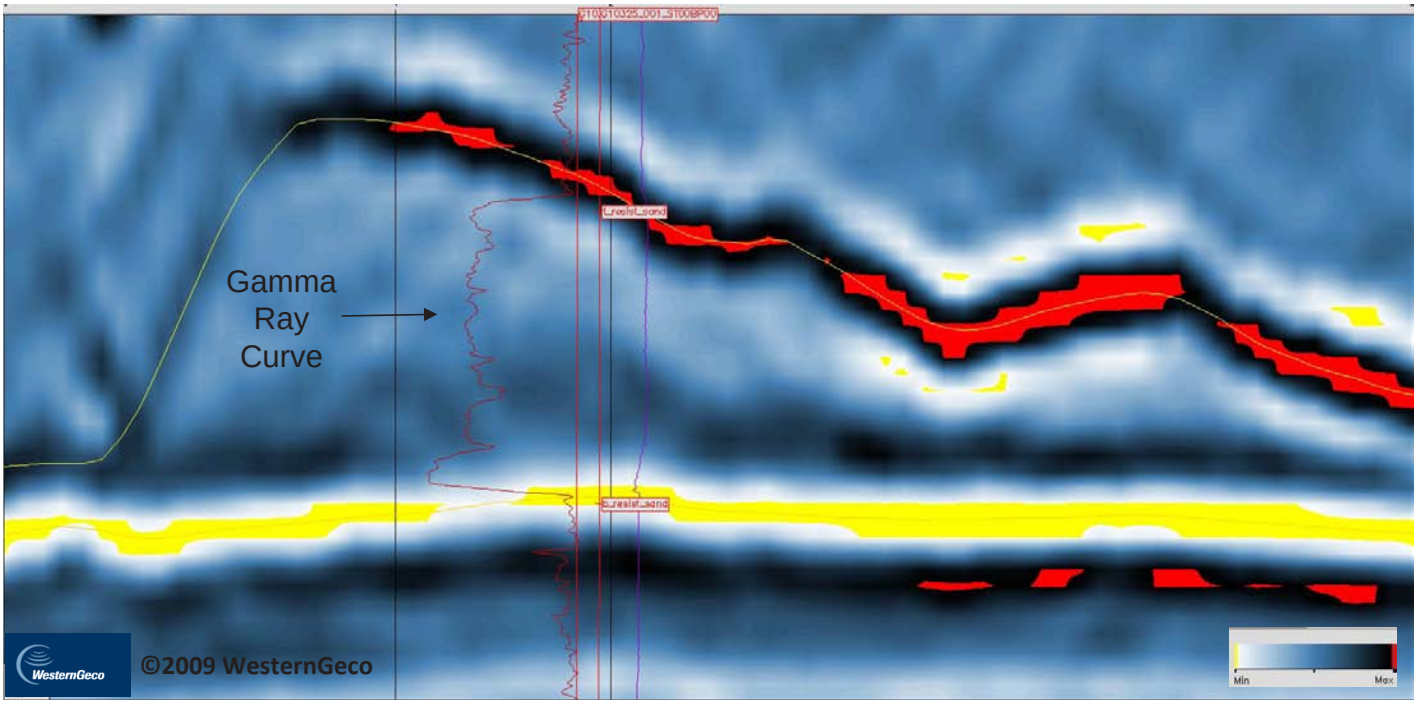

Figure F7: *Arbitrary seismic section through the EB 992 #001 well location. The top of the inferred sand corresponds to the strong seismic peak (red), and the base of the sand ties to the strong seismic trough (yellow). Sand interval measures 135 feet. Seismic data courtesy of WesternGeco.*

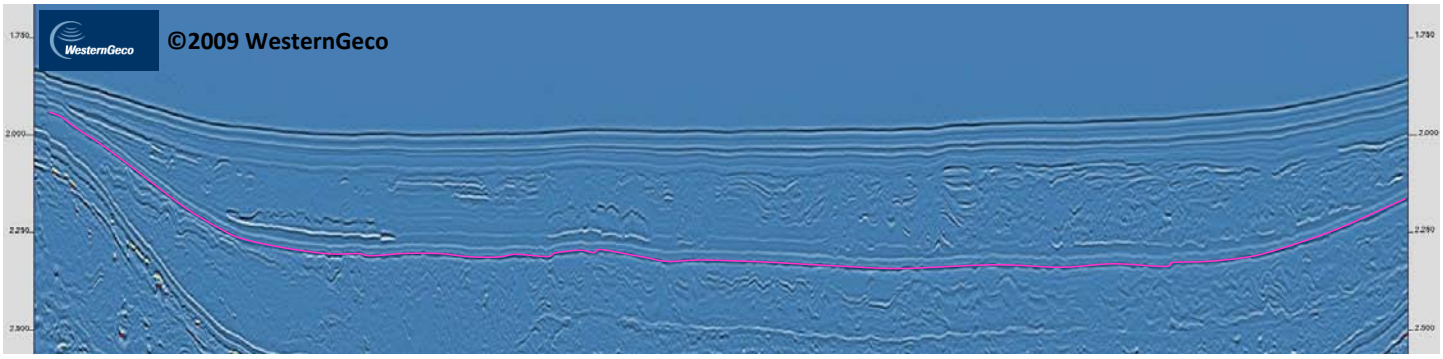

Figure F8: *Arbitrary seismic section showing stratigraphic location and basin-wide extent of Regional 1 horizon (magenta). Gas hydrate targets are stratigraphically above the Regional 1 horizon. Vertical axis is two-way travel time. Seismic data courtesy of WesternGeco.*

non-bedded features. This interval is interpreted to contain sand-poor mass transport and mass wasting events. The base of gas hydrate stability is predicted within this interval and is sometimes interpreted to be coincident with the strong trough reflector in the middle of Unit 5.

The stratigraphic units described above and identified in Figure F6 represent a slightly-finer subdivision of facies (based largely on seismic character) than the logging units presented by Guerin *et al*. (2009). Our stratigraphic Units 1 and 2 comprise the single Logging Unit 1 described by Guerin *et al*. (2009); our stratigraphic Unit 3 is equivalent to Logging Unit 2; our stratigraphic Unit 4 is equivalent to Logging Unit 3; our stratigraphic Unit 5 is equivalent to Guerin *et al*. (2009) Logging Unit 4.

The regional seismic stratigraphic signature of the gas hydrate target interval in the Diana basin (as seen in the EB 992 #001 well) is best characterized by evaluating a window of amplitude response above the Regional 1 horizon. The amplitudes within this window, which includes both top and base reflections, provide a detailed image of the areal distribution and morphology of stratigraphic Unit 3. By mapping these regionally extensive reflectors, we are also able to assess nature and extent of faulting in the shallow section. For a quick-look approach, we also extracted a suite of attributes in a window that extends 150 milliseconds (ms) two-way travel time above the regional horizon. Figure F9 is a rendering of the root mean squared (RMS) amplitude, a seismic attribute which incorporates the magnitude of both the peak and trough amplitudes. The RMS amplitude extraction highlights those areas (within the 150 ms window of investigation) that contain both strong peak wavelets and strong trough wavelets by calculating the square root of the mean of the squares of the values, shown in the following equation:

$$x_{\text{rms}} = \sqrt{\frac{1}{n}\sum_{i=1}^{n} x_i^2} = \sqrt{\frac{x_1^2 + x_2^2 + \cdots + x_n^2}{n}} \quad \text{.... Equation 1}$$

The industry wells in Table T1 provide critical calibration points to the RMS amplitude display, and lead to the interpretation of at least two Upper Pleistocene depositional facies that are associated with the lowstand deepwater fan deposits in our stratigraphic Unit 3. The description of each includes facies assemblages that can often be segregated at the local or prospect level, but we are limited in our general knowledge of the stratigraphic architecture in the Upper Pleistocene to only those wells that logged the section. Further, we have no core through these intervals, inhibiting interpretations at the bedding-scale level. Our Facies "A" and "B" described below are similar to older and deeper depositional facies in the Diana basin described by Sullivan and Templet (2002).

Facies "A" - Proximal Channel Axis: The Upper Pleistocene target section seen in the EB 994 and 990 wells is a complex arrangement of both blocky and fining-up sand sequences that likely are the result of several depositional events. However, the collective assemblage at each is interpreted to reflect deposition in a mostly-axial channel facies proximal to the source, where the blocky sands are likely to be high-concentration turbidites in a confined setting, and the fining-up sand sequences reflect waning flow and channel fill. Often, deepwater channel sand bodies of these architectures are found in close association and reflect axis to margin changes in amalgamation and lithofacies (Sullivan and Templet, 2002).

The corresponding RMS amplitude display (Figure F9) reveals a prominent SW/NE trending anomaly in the northern part of the basin (penetrated by the EB 990 #001 well), interpreted to represent a relatively long-lived channel axis capable of delivering sediment to the distal parts of the basin. This feature measures between 2.5 and 5 miles wide, over 8 miles in length, and is highly variable in thickness. A second proximal channel axis is inferred from the lithofacies assemblage in the EB 994 #001 well and from the RMS display, where the seismic amplitude response builds in a basinward direction.

Facies "B" - Distributary Channel Complex: The gas hydrate target sand in the EB 992 #001 well contains a sharp base and a sharp top, with minimal shale breaks, and no appearance of fining- or coarsening upward trends. This response is similar to some of the log characteristics noted in Facies A, but the vertical extent of sand present suggests a more distal distributary environment. We interpret the depositional environment at this location to be axial channel facies of high-volume distributary complexes located in a mid-fan environment.

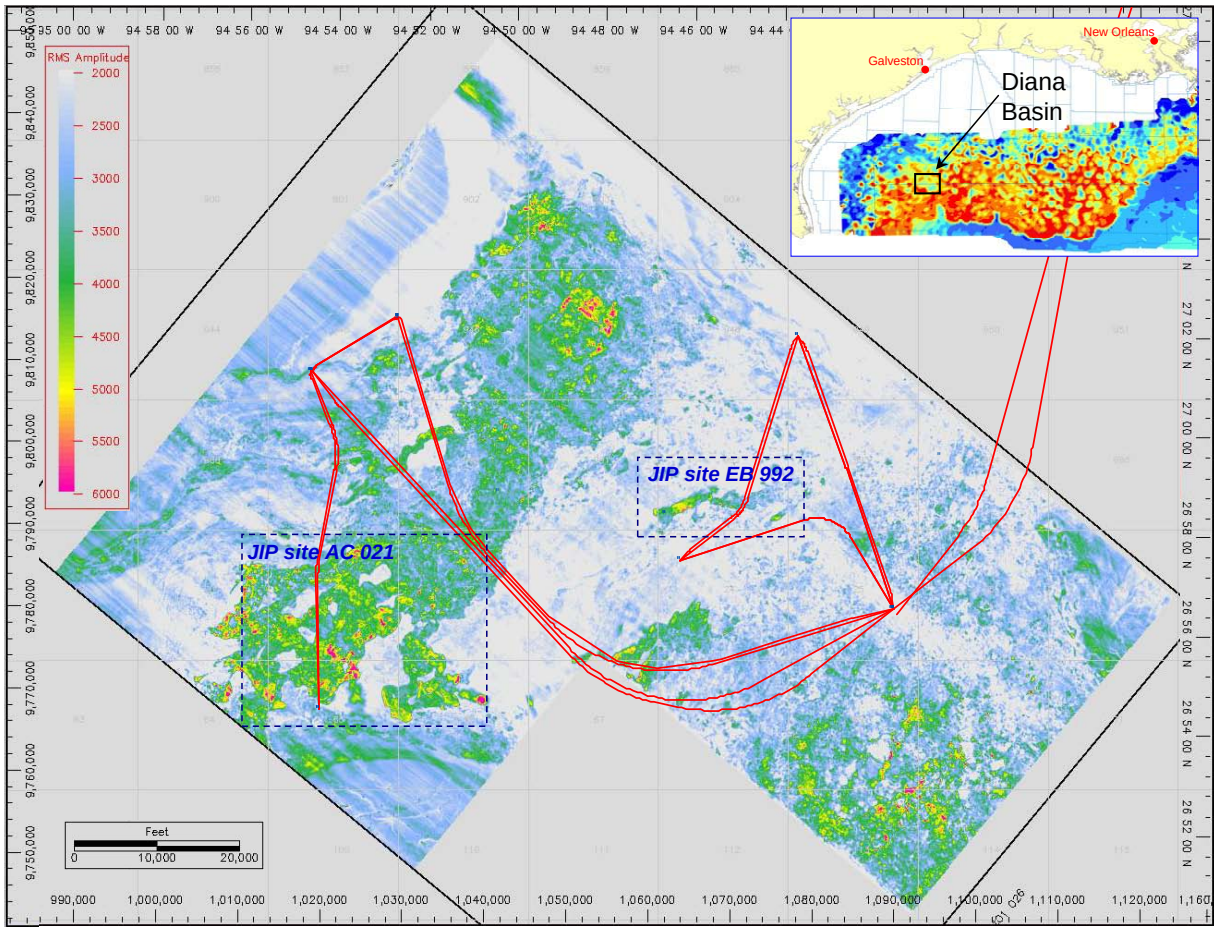

Figure F9: *RMS amplitude extraction 150 milliseconds above Regional 1 horizon. Industry well penetrations (blue) and pipelines (red) shown for reference. Underlying data provided by WesternGeco.*

The EB 992 well penetrates the target section in an area of high RMS amplitude response. The geometry of the local RMS response is oriented in a nearly-linear, slightly sinuous west/east trend that spans nearly 15,000 ft in length and 1200 - 2000 ft in width. The amplitude varies in thickness at the local scale from less than 50 ft to greater than 200 ft. We interpret Facies B to display complex lateral heterogeneity, including channel margin and compensating distal lobe deposits of varying thickness, coarseness, and net to gross sand ratios. The AC 024 #001 penetrates the target section approximately one mile southeast of the EB 992 #001 well in an area of limited RMS response, where the gamma ray indicates relatively thin sands interbedded with marine shales. Also, the shale-dominated Upper Pleistocene section seen in the EB 945, 946, and AC 65 wells, comprising thin interbedded sands, is interpreted to represent distal channel, channel-margin, and limited sheet sand deposition.

Based on the distribution of proximal to distal depositional facies, the seismically-identified geometry of the various facies, and the structural configuration of the Diana basin as controlled by the modern emplacement of shallow salt features, we interpret two primary sediment entry points into the basin. These entry points are shown in Figure F10, labeled as North and East. Sullivan and Templet (2002) recognized these same approximate entry points as the source of the older reservoir facies seen in many of the producing fields in the Diana basin.

East Entry

Sullivan and Templet (2002) described whole core taken from the Hoover field (AC 25) reservoir as amalgamated proximal channel deposits sourced from the east entry point. The Lower Pliocene-age Hoover field reservoir (~3.6 *my*; Symington and Higgins (2000) is approximately 8000 ft deeper, and several depositional sequences older, than our target interval. However, we believe this sediment delivery system was still active during the Upper Pleistocene (< 0.44 *my*) and is the likely source of the sediment inferred

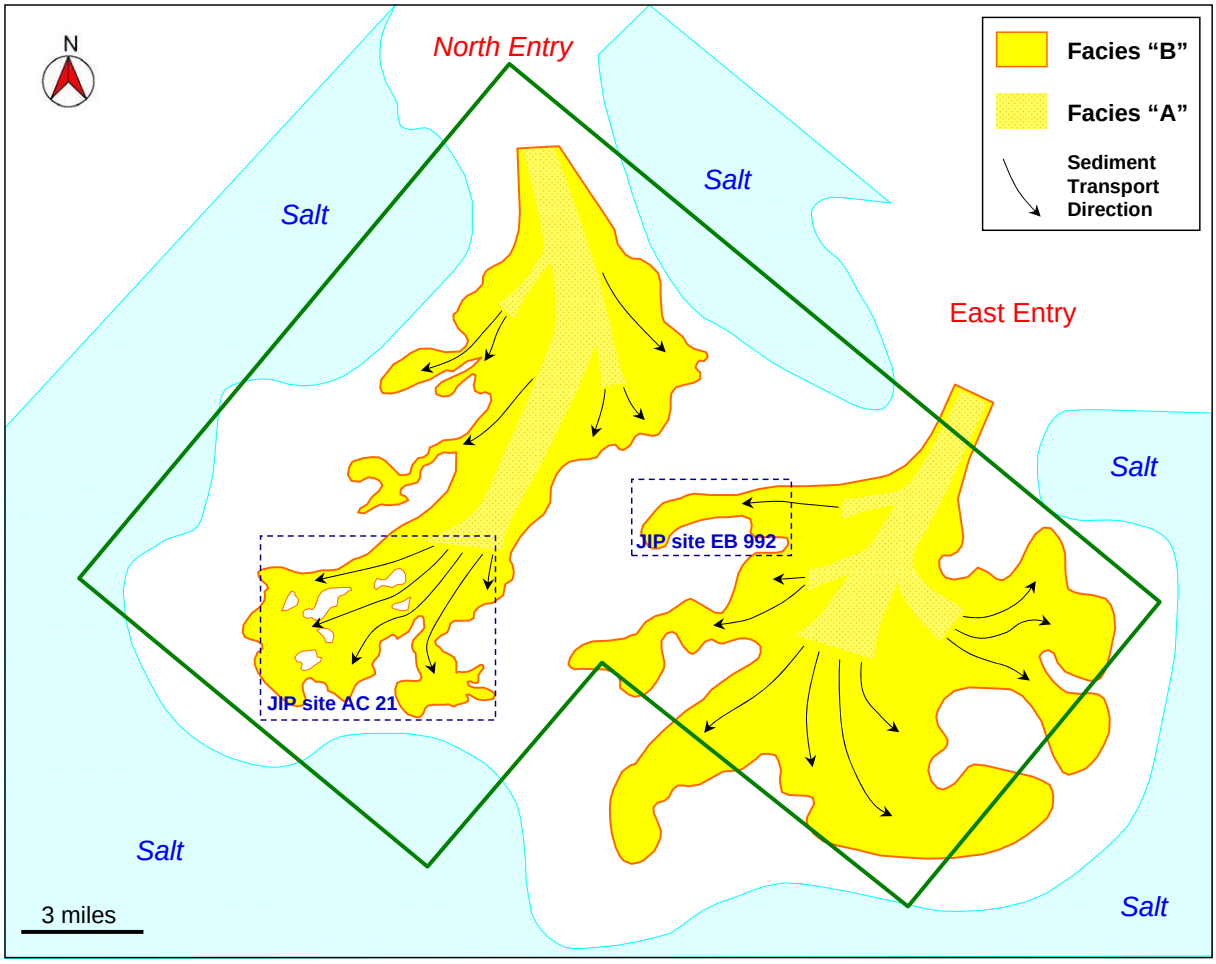

Figure F10: *Depositional system distribution based on seismic attributes and industry well penetrations. Dark green outline is approximate extent of East Breaks/Alaminos Canyon 8-Q multiclient 3-D Kirchhoff prestack time migration survey. JIP Leg II sites AC 21 and EB 992 in dashed polygons.*

to comprise the seismic amplitude response seen in the southern half of the basin, including EB 992 (Figures F9 and F10). Additionally, we believe that the thick (~450 ft) Upper Pleistocene sand sequence logged in the EB 994 #001 well was deposited in a very proximal position to the East entry point, resulting in amalgamated and stacked channel facies with high net/gross sand ratios. Incidentally, the RMS amplitude provides little seismic response at the EB 994 #001 well location and the Upper Pleistocene sands here are water-wet and non-gas hydrate bearing.

North Entry

Sullivan and Templet (2002) also described whole core taken from the Diana (EB 945) and South Diana (AC 65) producing reservoirs, and attributed both to the sediment source provided by the north entry point into the Diana basin. The cored reservoir from the Diana field is described as a series of 10 to 15 ft thick stacked, sharp-based fining-up channels, interpreted to be deposited as part of a weakly confined/distributary channel complex. The cored reservoir from the South Diana field is described as an aggradationally-stacked, non-amalgamated succession of high-concentration turbidites, sandy debrites, and laminated shales, and interpreted as a distal distributary lobe complex (Sullivan and Templet, 2002).

While the age of the reservoirs from the Diana and South Diana fields (middle Upper Pliocene, or ~3.0 *my*; Symington and Higgins, 2000) are older than the targeted Upper Pleistocene zone of gas hydrate occurrence, we believe that the sediment source of the north entry point was still active in the Upper Pleistocene. The RMS amplitude response and industry well penetrations, especially the EB 990 #001, provide evidence for a proximal to distal distribution of facies from east to west. The 500 ft sand in the target interval just above the Regional 1 horizon at the EB 990 #001 well location is interpreted to be a series of stacked and amalgamated channels in a confined axial

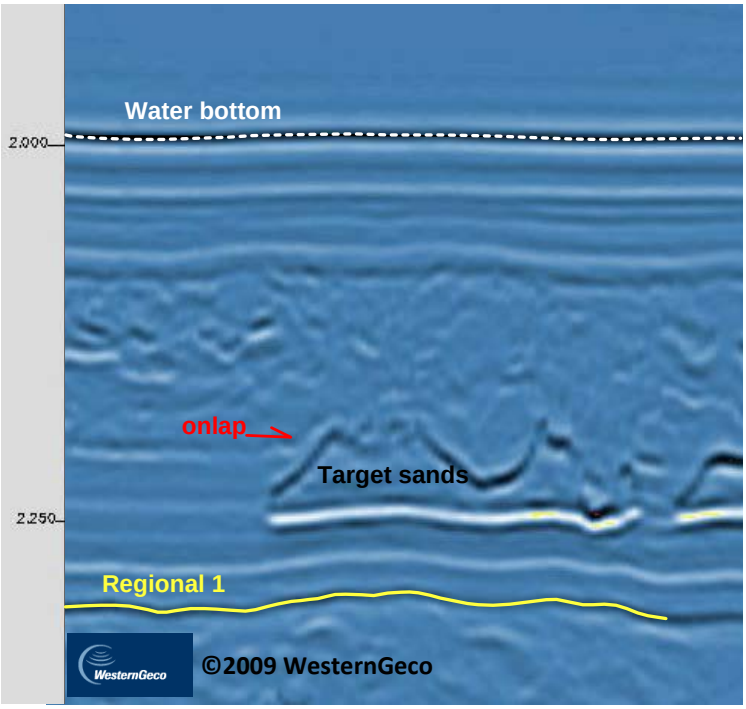

Figure F11: *Arbitrary seismic section showing constructional depositional geometry of target sand facies. Note onlap of subsequent drape deposits. Vertical scale is two-way travel time. Seismic data courtesy of WesternGeco.*

position, and relatively proximal to the sediment source. The RMS amplitude for this proximal channel facies often measures one half of the full scale, largely because the 150 ms window captures only the trough associated with the base of the channel sequence.

Several distal distributary channel and lobe complexes associated with the north entry are noted on Figure F10. Existing topography in the basin resulted in a focused distributary network of individual channel/lobe complexes on the order of ½ mile wide, with gross thicknesses greater than 150 ft in the weakly confined setting, and 50 ft thick in the less confined and more distal setting. While some basal scouring is noted on the seismic sections, many of the individual complexes are characterized by a flat base. Areas of non-deposition are noted where subsequent sedimentation, interpreted to be hemipelagic mud, drapes the relatively steep margins of the channel and lobe complexes (Figure F11).

Figure F12 is a strike section through the distal margin of the distributary complex in the AC 21 prospect area showing the compensatory nature of the lobe deposits. Also shown in this figure is a late stage mass transport complex/erosional event that has incised into an older lobe, highlighting the complexity of a long-lived sediment fairway. The late stage erosional nature of the system has incised many of the pre-existing depositional geometries.

Gas Source and Migration

Given the young age of the AC 21 reservoir system, a critical element of the overall petroleum system will be extent of potential gas charge. Two classes of gas source are considered; thermogenic sourcing from deeper systems (assumed to be those that charged the deeper producing fields in the basin) via observed migration pathways, and local biogenic sourcing.

In the northern Gulf of Mexico, major hydrocarbon systems are largely derived from thermally mature lower Tertiary, Upper Cretaceous, and Upper Jurassic source rocks (Hood *et al*., 2002). These source intervals are very old (between ~40 *my* and ~150 *my*), and in the western Gulf of Mexico they are buried at depths that typically range from 30,000 ft to 45,000 ft (Hood *et al*., 2002). Substantial vertical hydrocarbon migration is thought to occur through faults and fractures that coincide with the complex tectonostratigraphic interaction of relatively rapid sedimentation and vertical salt movement.

In addition to the abundant thermogenic hydrocarbons in the Gulf of Mexico, Milkov and Sassen (2001) report

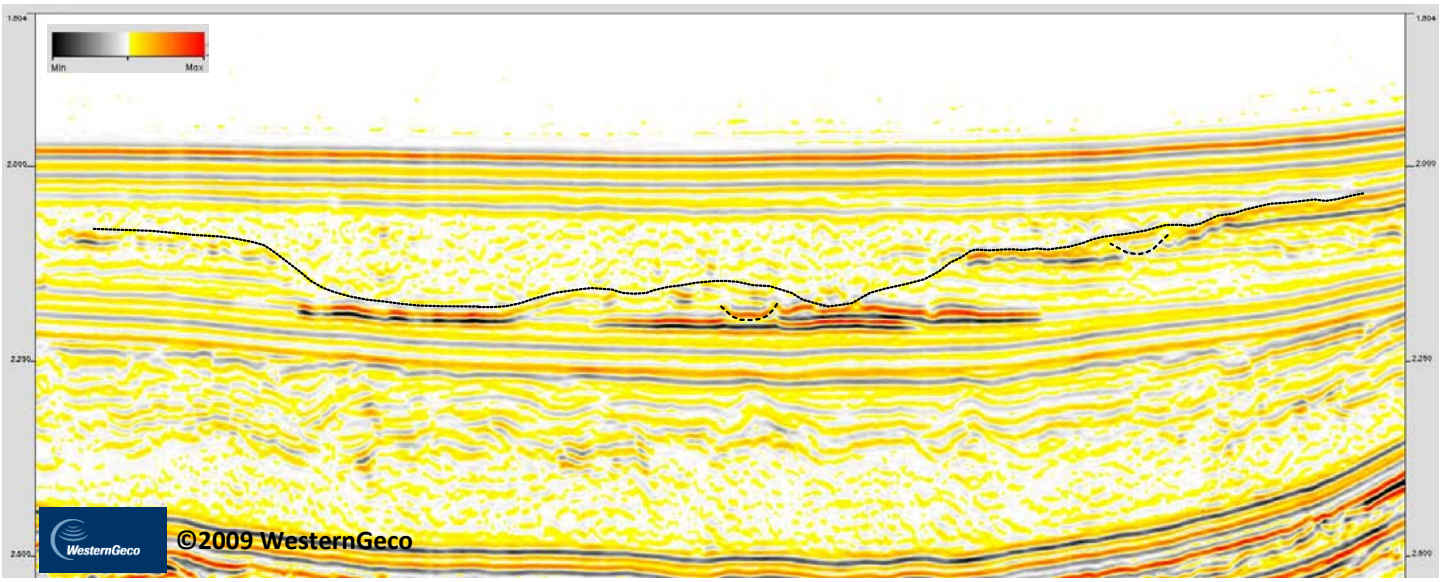

Figure F12: *Arbitrary seismic section through the distal margin of the AC 21 distributary lobe complex. Target facies exhibit relatively flat bases and lateral depositional extent on the order of 1 mile. Base of late stage erosional event/mass transport complex shown as black dashed line. Vertical scale is two-way travel time. Seismic data courtesy of WesternGeco.*

widespread shallow piston core evidence of biogenic methane that was generated through methanogenesis near the seafloor. The most recent assessment of in-place gas hydrate in the Gulf of Mexico (Frye, 2008) highlights both the availability of total organic carbon in the shallow section and the appropriate temperature conditions for microbial conversion to methane. Assuming a methane source entirely attributed to biogenically-generated gas, Frye (2008) reports a mean in-place gas hydrate resource of 21,444 trillion cubic feet (607 trillion cubic meters) in the Gulf of Mexico. Globally, many of the larger documented occurrences of marine gas hydrate systems have been shown to be of an entirely microbial origin, including those found off the east coast of the United States (Lorenson and Collett, 2000) and off the east coast of India (Collett *et al*., 2008).

Mechanism of gas charge to the hydrate stability zone in the Diana basin presented the greatest pre-drill risk as the most uncertain petroleum system element for the AC 21 Site. Unlike the H and Q targets at the GC 955 Site, which are located on three-way dipping fault traps over a broad area of four way closure (McConnell *et al*., 2009), the targets in the Diana basin are areally extensive deepwater fan deposits in basinal and basin-margin structural settings that remain distributed largely as depositional, rather than structural, events. Further, several of the industry well penetrations that recorded high-quality sand reservoirs in the hydrate stability zone (i.e. EB 990 and EB 994) are water-bearing with no evidence of gas charge.

Gas Hydrate Occurrence

The pre-drill integration of all available geological and geophysical information provided a moderate- to high-degree of confidence that gas hydrate would be present in the sand-rich reservoirs of stratigraphic Unit 3 throughout the Diana basin. The primary evidence for this interpretation includes the strong leading seismic peak correlative with the top of the unit and the elevated resistivity in the only pre-existing well to have tested the target facies (the EB 992 #001 well).

The top of the 135 ft-thick slightly resistive sand interval in the EB 992 #001 well appears to correlate to the strong seismic peak event on the 3-D seismic data, while the base of the sand ties to the strong seismic trough event (Figure F7). The nature of the peak over trough acoustic relationship is consistent with the presence of pore-filling gas hydrate at low to moderate saturations. Strong peak amplitudes have been successfully used to help identify gas hydrate reservoirs in the Milne Point area on the North Slope of Alaska (Inks *et al*., 2009) and at AC 818, south of East Breaks in the Gulf of Mexico (Boswell *et al*., 2009b). However, it should be noted that in the shallow

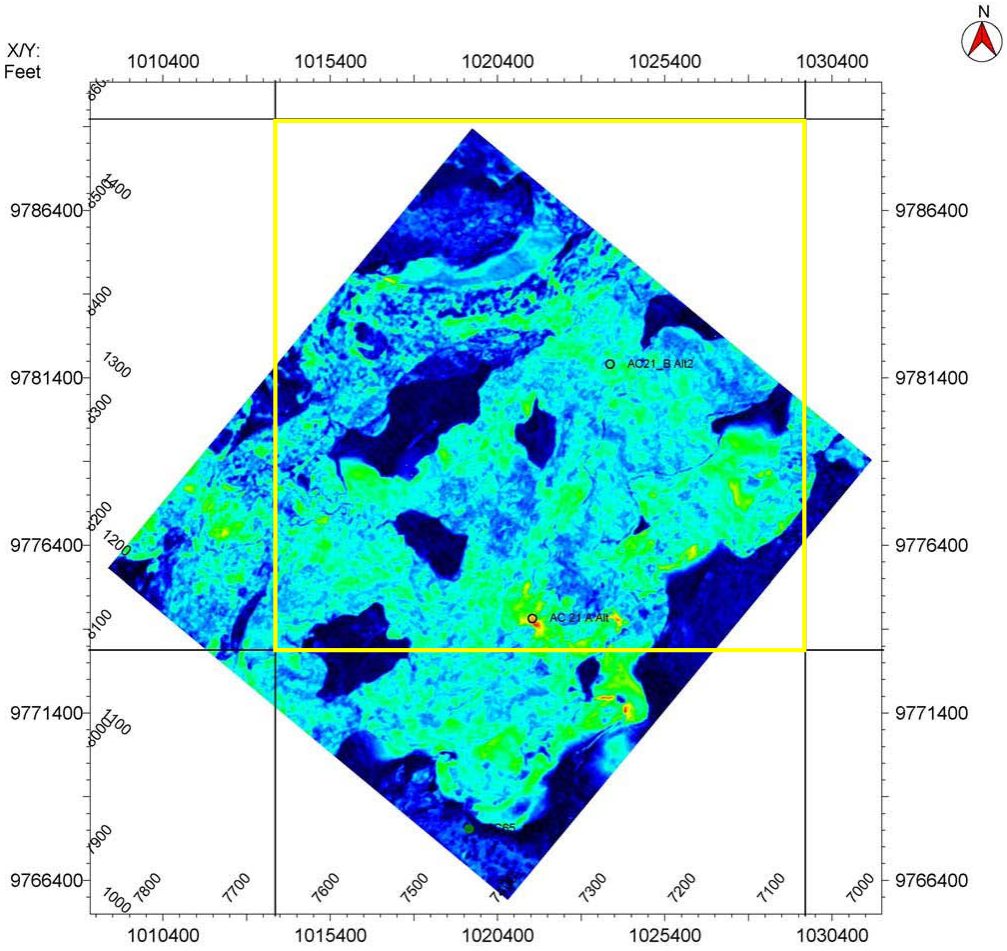

Figure F13: *RMS amplitude display across Site AC 21. GOM JIP Leg II well locations A and B and AC 65 #001 industry well are shown on the map. OCS block AC 21 measuring 3 miles x 3 miles is highlighted in yellow. Seismic data courtesy of WesternGeco.*

stratigraphic section of the Gulf of Mexico, the *p*-wave velocity of water-bearing sands may be greater than that found in surrounding shales (Gregory, 1977). The reflection coefficient between an assumed overlying shale and underling water-saturated sand at 350 fbsf is ~0.15 using velocities and porosities by Gregory (1977); this indicates a significant positive amplitude response from wet sands at this depth. As the depth of a sand reservoir increases the refection coefficient decreases and becomes negligible at about 1,500 fbsf. This illustrates that the interpretation of the leading peak amplitude from the reservoir alone to infer gas hydrate occurrence requires a careful consideration. An interval *P*-wave velocity at the EB 992 #001 well location was estimated at 6750 ft/s (2,057 m/s) on the basis of the thickness of the sand from the log and two-way travel time from the seismic data.

Site Selection

A total of seven wells at two sites in the Diana basin were permitted for Leg II drilling operations. The three wells permitted at the AC 21 Site were designed to test proximal to distal depositional facies associated with the distributary channel/lobe complex shown in Figure F13. Well locations were selected to allow for a maximum penetration thickness of the gross sand interval, as defined by the peak-leading seismic top and the basal trough reflector, and to provide a lithologic calibration to the seismic facies analysis. Changes in seismic amplitude response were attributed to the tuning thickness of the target sands (calculated to be ~40 ft), rather than to variations in S_{gh}. Because of this, spatial variability of S_{gh} was not predicted pre-drill, as the seismic attribute response was largely ubiquitous across the AC 21 target area. Specifically, the AC 21-A well location was selected to evaluate two closely-spaced peak/trough pairs at the target horizon level. This dual relationship is

not widely distributed across the target area. The AC 21-B location was selected to test a thick interval in a proximal position of the distributary system. The AC 65-A location was permitted to test distal lobe facies that mark the presumed termination of the depositional system, where the gross target interval measures ~75 ft thick. The two wells (AC 21-A and -B) at this site that were drilled are discussed in the ***Site AC 21 Drilling Results*** section.

Four wells were permitted to drill during Leg II operations at the EB 992 Site (Shedd *et al*., 2009b). The EB 992-A was permitted several hundred feet up-dip from the EB 992 #001 industry well in an effort to acquire high-quality LWD data in close proximity to the existing EB 992 #001 log suite. EB 992-B was permitted to test a moderately thick target sand (~120 ft) where the basal trough reflector exhibits a possible seismic "pull-up" phenomenon. Seismic pull-up typically occurs beneath a feature comprising anomalously fast acoustic properties; in this case, believed to be associated with anomalously high gas hydrate saturation. Location EB 992-C was selected to test the near-maximum thickness of the target sand in the EB 992 vicinity, here measuring in excess of 200 ft. Finally, the EB 992-D location was permitted in an area of relatively thin target thickness (< 60 ft) and high acoustic amplitude in a test designed to calibrate the pre-drill seismic tuning thickness model.

Operations

During the first week of May 2009, two of the three permitted wells at Site AC 21 were drilled utilizing the Helix *Q-4000* semi-submersible drilling rig (Boswell *et al*., 2009a). For a complete operational summary of these two wells - the AC 21-A and AC 21-B - see Collett *et al*. (2009b). Preliminary results from these two wells are presented in the ***Site AC 21 Drilling Results*** section and in Guerin *et al*. (2009). The AC 65-A location was not drilled due to time and budgetary constraints and the determination that the AC 21-A and -B wells had adequately tested the geologic concept that the JIP had desired to test at the AC 21 Site (Boswell *et al*., 2009a).

None of the four permitted well locations at Site EB 992 were drilled during Leg II (Boswell *et al*., 2009a). In short, a moored deepwater drilling vessel was on station in the immediate vicinity of our well locations, with anchors deployed to the seafloor that served to obstruct our direct access to several of the permitted locations.

AC 21 Drilling Results

Hole AC 21 - A

Water depth = 4940 fbrf; target sand depth = 5480 fbrf; well total depth = 6700 fbrf

The AC 21-A well was the first location drilled at the AC 21 Site and penetrated what we believe to be the entire gas hydrate stability zone to a total depth of 6700 ft below rig floor (fbrf, Figures F14 and F15). The height of the rig floor is 51 ft above sea surface at the AC 21-A location. The base of gas hydrate stability (BGHS) was anticipated at 6474 fbrf (1534 fbsf). The BGHS is not observed as a seismically-defined feature at this location.

The upper 540 ft of the well logged a mud-prone section comprising shales and interbedded silts with a relatively uniform gamma ray response (Figure F16). This zone is marked by a linear increase with depth of both resistivity and velocity, and corresponds to stratigraphic Units 1 and 2, as described from Figure F6.

Per drilling standards set for the entire Gulf of Mexico JIP Leg II drilling program (Collett *et al*., 2009b), the rate of penetration at the bit was slowed above the targeted sand interval from approximately 350 ft/hr instantaneous to 180 ft/hr instantaneous. The target sand (Stratigraphic Unit 3 on Figure F6) was encountered at a depth of 540 fbsf. The gross target interval, as defined by a leading seismic peak and a lower seismic trough, consists of two well-defined sand units separated by a 15 ft shale break. The upper sand unit is 15 ft-thick with a rather sharp base and top. The lower sand unit is 62 ft-thick and contains a sharp base and a slightly-fining up top. Based on gamma ray response, the ratio of sand to shale in both of the target sands is very high. Both the upper and lower sand units contain measured resistivity's that only slightly exceed 2 Ω-m at the maximum value. The resistivity in the lower sand unit measures 2 Ω-m for the upper 20 feet, then decreases in the lower 45 feet to 1.5 to 2 Ω-m. The compressional velocity measured by the MP3 tool indicates greater velocities in the target sands than in the surrounding shales. However, the velocity measured by the sonicVISION tool does not display any matching increase.

The AC 21-A well was drilled in gauge at 8.5 inches for all parts of the hole except the upper 220 fbsf, and in

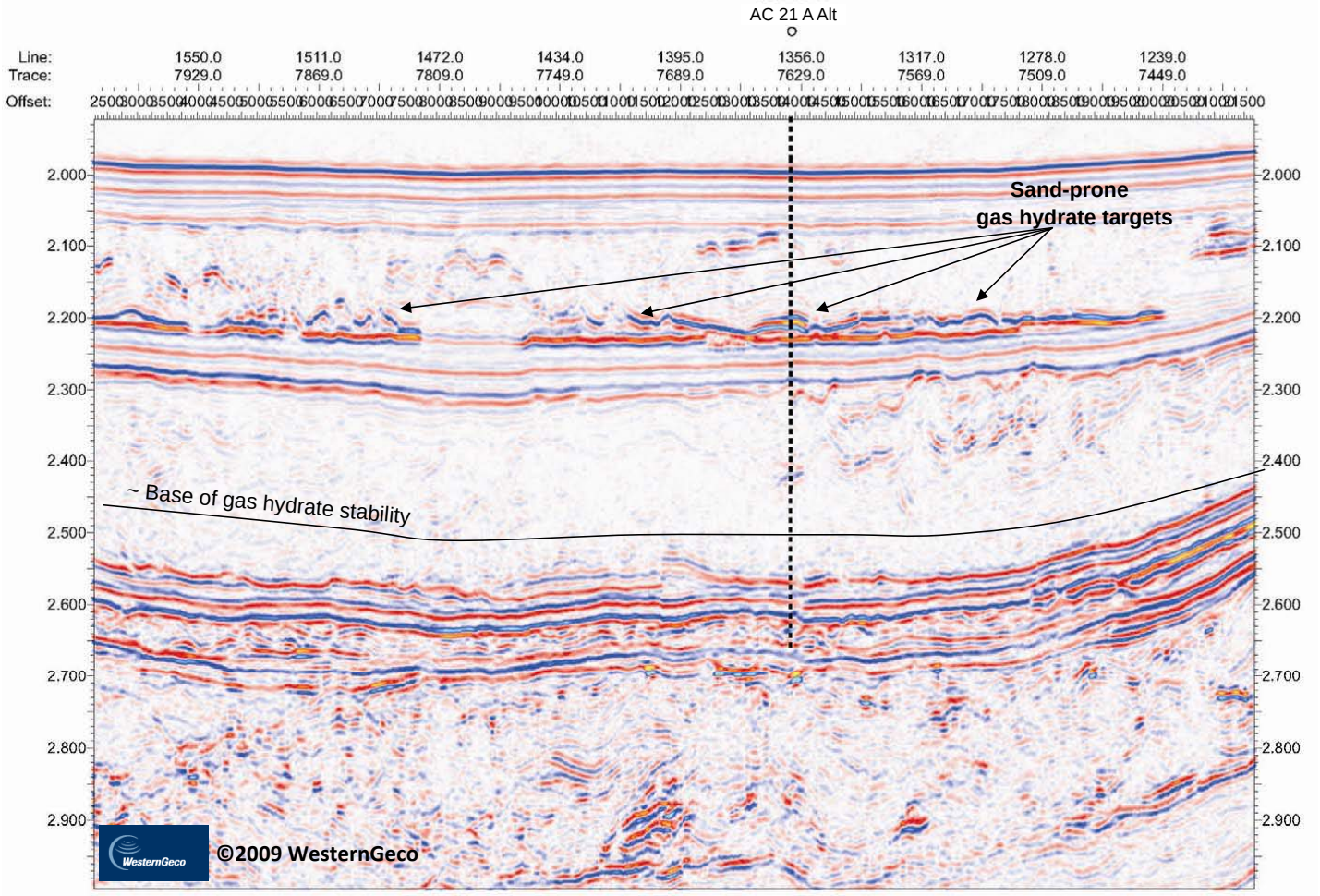

Figure F14: *Arbitrary seismic section through AC 21-A well. Vertical scale is two-way travel time. Seismic data courtesy of WesternGeco.*

the target sands interval identified above, where caliper measurements indicate extensive washouts to 10 inches. Because of this, some of the recorded data in these intervals, particularly density and porosity, are unreliable and are not reported on here.

The section immediately below the target sand comprises a 105 ft-thick shale interval underlain by an approximately 100 ft-thick section of laminated sands, silts, and shales (collectively stratigraphic Unit 4 on Figure F6). The resistivity of the laminated sands, (~1.0 Ω-m) is slightly less than the overlying shale (1.5 Ω-m).

The lithology in the bottom ~10,00 ft of the hole is shale -dominated and marked by very little inflection from the baseline gamma ray response. However, an anomalously resistive section nearly 260 ft-thick deviates from the baseline resistivity beginning at 1252 fbsf, moving from a background resistivity of 2 Ω-m above the break to between 2 and 3 Ω-m in the anomalous zone. This zone of increased resistivity is marked by only a slight inflection in both formation density and acoustic velocity from the baseline. The resistivity of the final 180 ft shale section at the bottom of the hole returns to background values of 2 Ω-m. This entire shale-dominated interval is equivalent to stratigraphic Unit 5 on Figure F6.

Hole AC 21 - B

Water depth = 4934 fbrf; target sand depth = 5452 fbrf; well total depth = 6050 fbrf

The AC 21-B well was the second location drilled at the AC 21 Site during Gulf of Mexico JIP Leg II. The well was stopped short of the permitted total depth of 6975 fbrf (2041 fbsf) and the presumed BGHS (6475 fbrf; 1541 fbsf) due to both project logistics and the absence of sand-prone facies at these depths in the AC 21-A well. The calculated BGHS is not observed as a seismically-defined feature at the AC 21-B location (Figures F15 and F17).

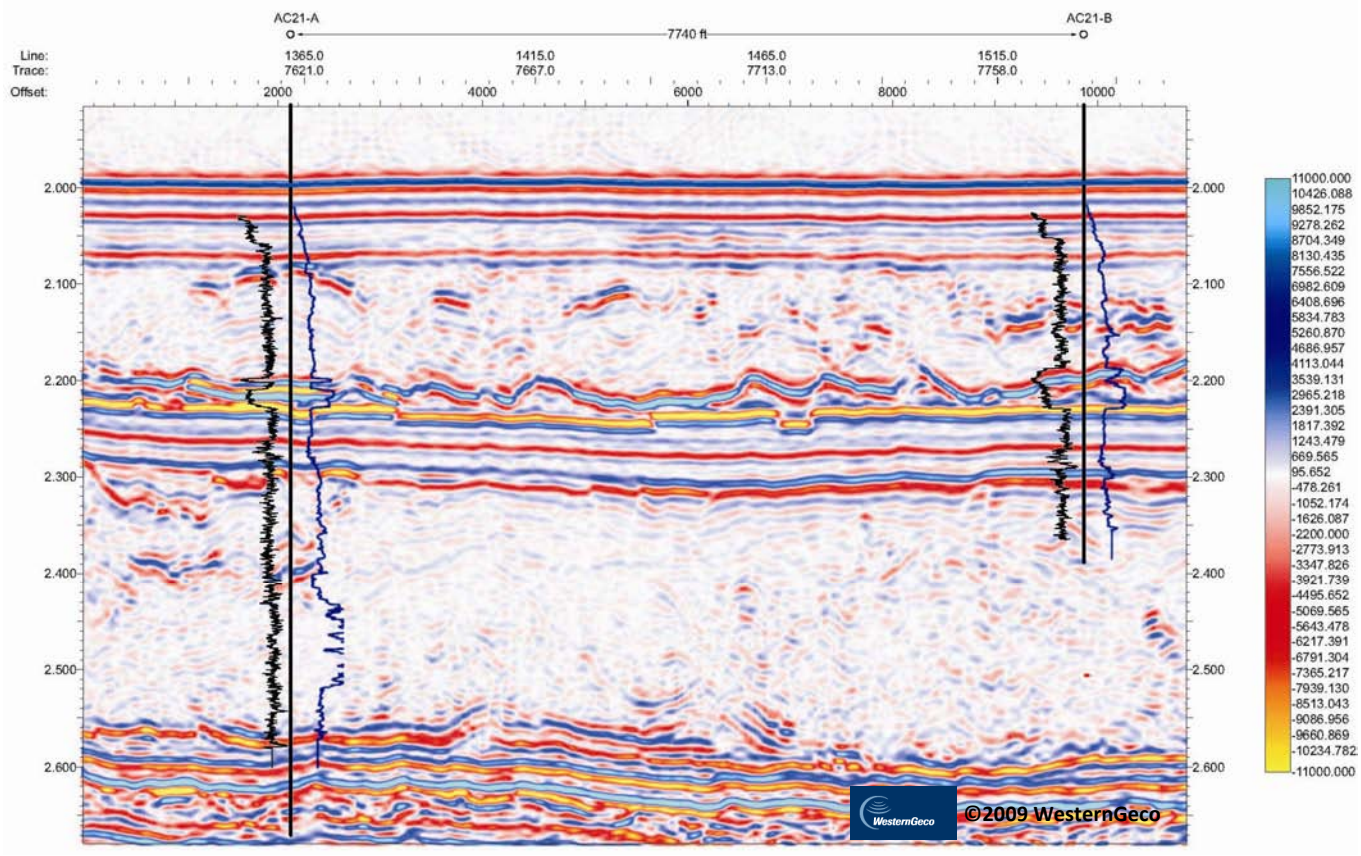

Figure F15: *Seismic section through AC 21-A and AC 21-B wells. Gamma ray (left) and resistivity (right) log curves are superimposed. Vertical scale is two-way travel time. Seismic data courtesy of WesternGeco.*

The AC 21-B location is located ~1.45 miles northeast of the AC 21-A location (Figure F13). As expected, the logged interval is of a very similar character to that seen in the AC 21-A well, with the exception of the geometry and thickness of the sands at the target interval (Figure F18).

The target sand was encountered at a depth of 518 fbsf. The gross target interval, as defined by a leading seismic peak and a lower seismic trough, consists of a single sand unit of slightly varying gamma ray response. The total gross thickness of the sand is 125 ft with no obvious shale breaks, yielding a net/gross sand ratio of nearly 100%. The sand package can be further divided into two informal units: a lower unit ~80 ft-thick with a blocky gamma ray log character, and an upper unit ~45 ft-thick with a slightly cleaner base and shaling-upwards log character. Formation resistivity in the target sand is approximately 2 Ω-m (similar to that described in the AC 21-A well), except for the cleaner sands in the upper unit where resistivity measures ~1.5 Ω-m. Overall, the MP3 compressional velocity (V_p) data throughout the target sand interval tracks the general velocity trend of increasing transit time with depth. However, small inflections within the sand tend to track the resistivity measurements, where higher velocities are associated with zones of higher resistivity.

The AC 21-B well was drilled in gauge at 8.5 inches for all parts of the hole except the upper ~140 fbsf, and in the target sand between 520 and 650 fbsf, where caliper measurements indicate extensive washout to 10 inches. Because of this, some of the recorded data in these intervals, particularly density and porosity, are unreliable and are not reported on here.

The section immediately below the target sand comprises a 125 ft-thick shale interval underlain by an approximately 120 ft-thick section of laminated sands, silts, and shales. The well reached a total depth of 1116 fbsf (6050 fbrf) in shale.

Gas Hydrate Occurrence

The available data for the wells in the AC 21 site are consistent with the occurrence of pore filling gas hydrate

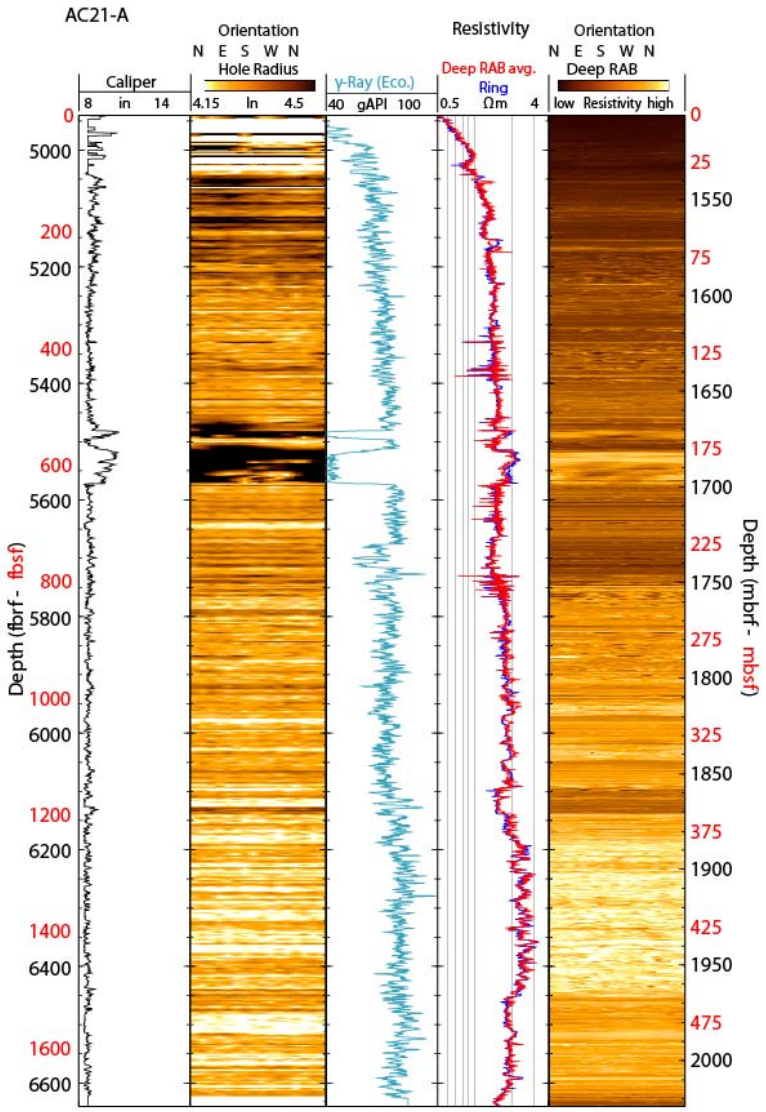

Figure F16: *AC 21-A well LWD data.*

at moderate to low concentrations. Elevated formation resistivity in the target sands (> 2 Ω-m) compared to that in nearby water wet sands in the basin (< 1.0 Ω-m) suggests maximum gas hydrate saturation (S_{gh}) estimates up to 50% (Guerin *et al*., 2009) using both Archie's equation and the quick look technique. Also, processed LWD acoustic data from the MP3 indicate a slight increase in compressional velocity through the resistive sections of the target sands. This slight measured velocity increase is in agreement with recent work (as compiled in Waite *et al*., 2009) that suggests low concentrations of S_{gh} would be accompanied by only a negligible or modest increase in sediment velocity.

Figures F19 and F20 show gas hydrate saturation plots for the target sands in the AC 21-A and -B wells, respectively. In these examples, hydrate saturation was calculated using the quick look method with a background resistivity value of 0.9, yielding S_{gh} estimates that range from approximately 20% to 40% of the pore volume. This background resistivity (0.9) is the lowest measured resistivity from a slightly cleaner clay interval at 737 fbsf in the AC 21-A well and at 778 fbsf in the AC 21-B well (Figures F16 and F18). Using a more conservative approach, S_{gh} was also calculated using the background resistivity value of 1.5 Ω-m that reflects the resistivity of the clay sediments in the well and yields hydrate saturations between 0 and 20%. Saturation estimates are presented for *n* values of both 1.5 and 2.5.

In addition, the elevated resistivity in the deep shale section at AC 21-A (Figure F16) is also interpreted to potentially represent low gas hydrate saturation, although additional evidence such as high acoustic velocity and images of fracture fill (from the geoVision) are not widely observed

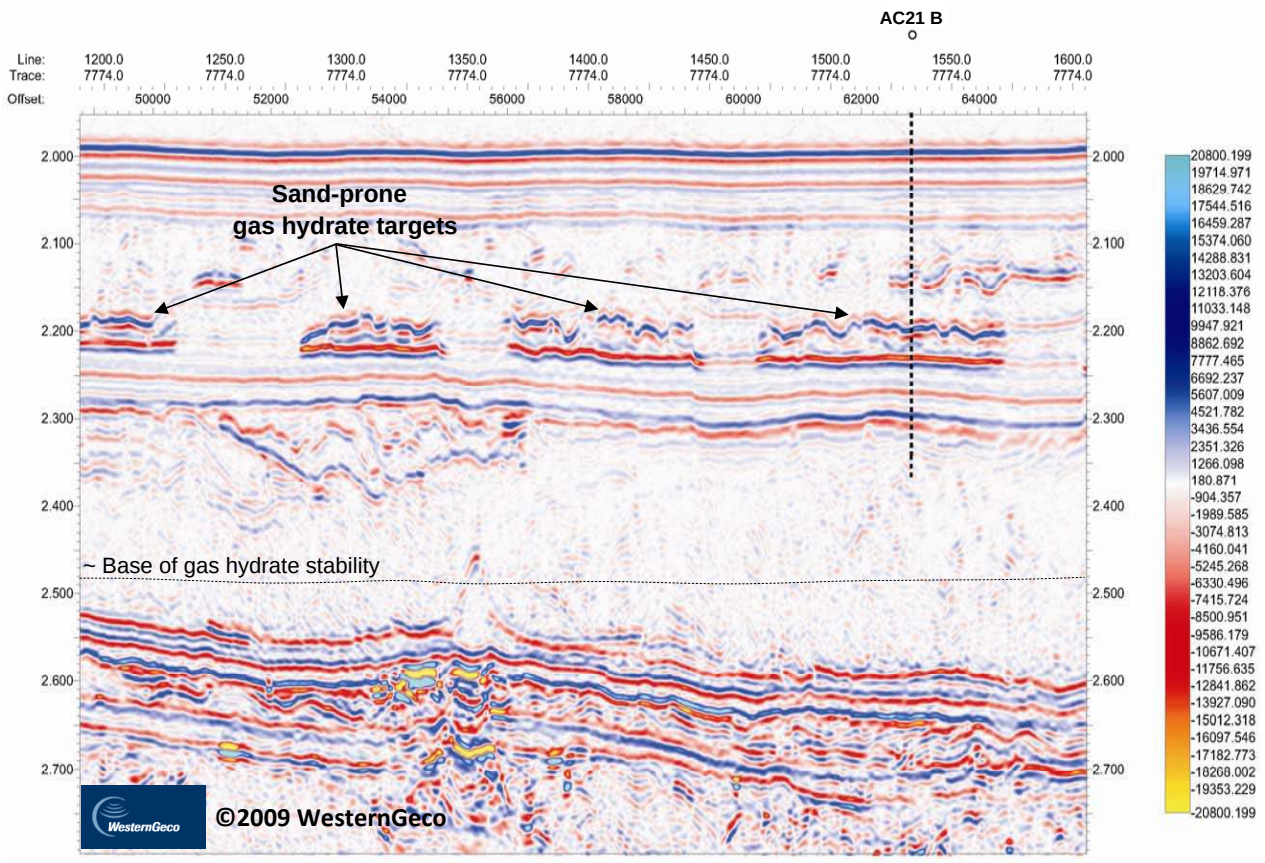

Figure F17: *Arbitrary seismic section through site AC 21-B well. Seismic data courtesy of WesternGeco.*

(Guerin *et al.*, 2009). Solving Archie's equation with an *m* value of 2 yields S_{gh} estimates of 20-30% throughout this 260 ft gross shale interval (Guerin *et al*., 2009), however, it is well recognized that application of Archie's to non-pore-filling gas hydrate can lead to significant errors (Hadley *et al*., 2008; Lee and Collett *et al.*, 2009).

The absence of any clearly water-wet sands in the AC 21-A and -B wells limits our ability to precisely calibrate the anomalous log response in the presumed gas hydrate-bearing target sands to background log values in the immediate vicinity of the wellbore. Coeval water-bearing sands are present in the EB 990 #001 well less than 6 miles (10 km) away, but the petrophysical measurements were acquired in a much larger borehole designed to evaluate a deeper, conventional target. Also, the relatively unconsolidated nature of the shallow gas hydrate target sands allowed for significant borehole enlargement through the objective, and the resulting formation density measurements are thought to be adversely affected.

Discussion

The JIP Leg II wells at AC 21 confirmed our pre-drill interpretation of a widespread Upper Pleistocene sand-rich depositional system across the target area in the Diana basin. Peak-leading seismic events mark the top of high net/gross sand bodies. The basal seismic trough observed at each well location marked the base of the target sand interval.

The lower target sand (62 ft-thick) in the AC 21-A well and the entire 125 ft-thick target sand in the AC 21-B well are interpreted to be genetically related as part of the same depositional event or events. With the relatively uniform character of the gamma ray response and the absence of any clear shale breaks in the sand interval, it is difficult to characterize the nature or presence of the highest frequency depositional events. Certainly, the log record does not appear to indicate a strong lateral shift in depositional facies, and only a hint of amalgamation of like facies, as seen at 564 fbsf in the AC 21-B well. Based on the log response, the areal seismic attribute distribution, and the vertical relationships described earlier from the seismic

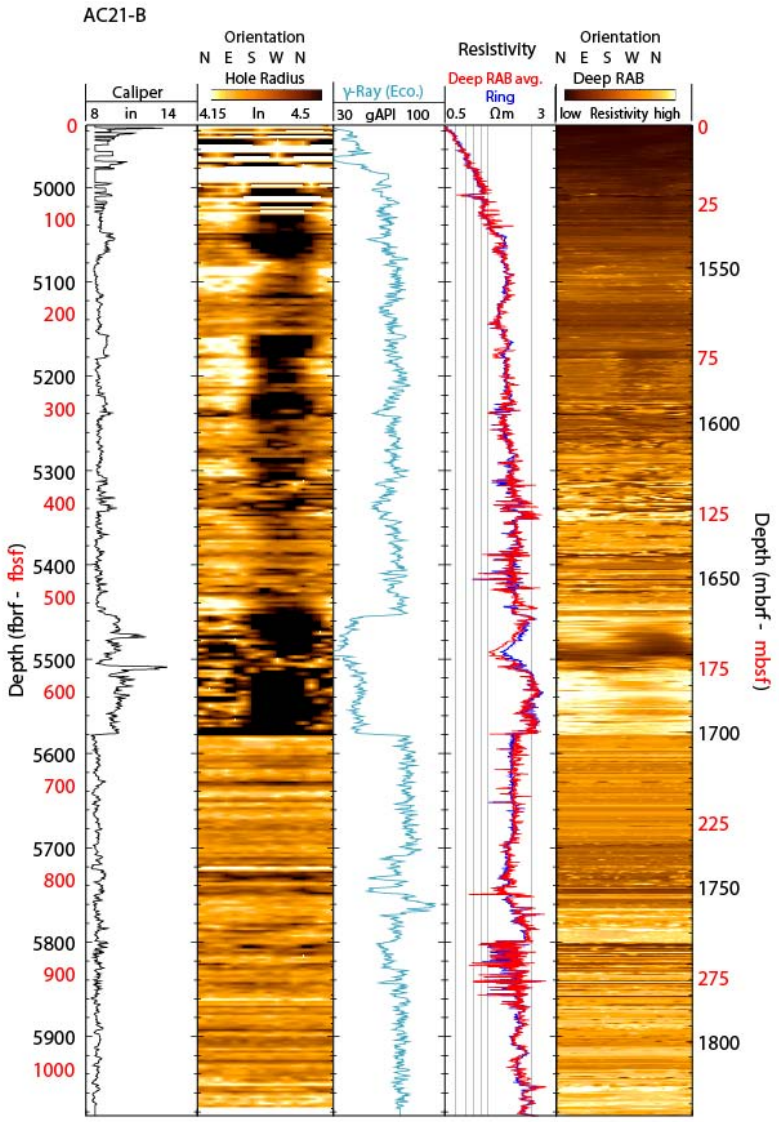

Figure F18: *AC 21-B well LWD data.*

data, these target sands are interpreted to have been deposited by a relatively short-lived, sand-rich deepwater delivery system. The architecture of the lower sand unit is complicated such that in many areas the top of the sand appears to have a constructional nature with a convex top, while in areas such as the AC 21-A well location, younger erosional events have left a concave top and an incomplete lower sand unit.

The upper target sand (15 ft-thick) in the AC 21-A well is interpreted to comprise the basal sandy member of a younger mud-prone mass transport complex. Here, we observe significant downcutting through as much as 400 feet of section, terminating at the stratigraphic level of the lower target sand. As this gross younger system is more mud-prone, the upper target sand in the AC 21-A well is not interpreted to be widely distributed across the AC 21 target area, but possibly only in those areas of maximum incisement (the axial position). The presence of the upper target sand does appear predictable as the seismic data response at the AC 21-A location reveals two distinct (and anomalous) peak/trough pairs. The dual amplitude response is not widespread across the target area.

Many chronologic, lithologic, and depositional similarities are noted between the gas hydrate target section in the Diana basin and the shallow section (< 1000 fbsf) of the well-studied Brazos-Trinity Basin IV (e.g., Flemings *et al*., 2006; Mallarino *et al*., 2006; Beaubouef *et al*., 2003; Beaubouef and Friedmann, 2000), which is located ~40 miles northeast of the Diana basin. Here, interbedded deepwater sands and shales are described through the

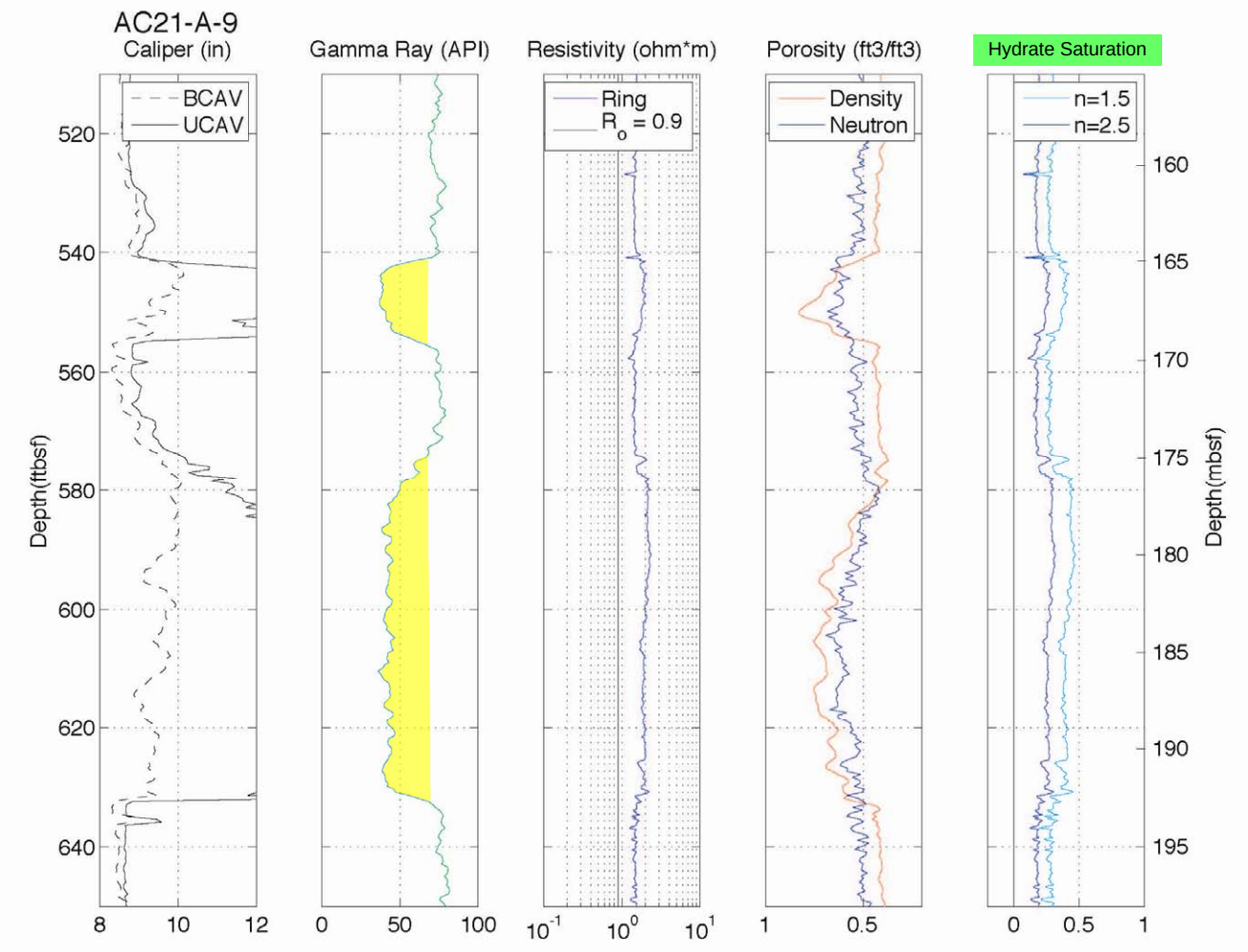

Figure F19: *Calculated gas hydrate saturation, AC 21-A well using Archie's quick-look method for two assumed values for exponent n (Guerin et al., 2009).*

analysis of whole core, piston core, and well log data, including a gross sandy interval in excess of 300 ft in the axial margin of the basin (Flemings *et al*., 2006). Beaubouef and Friedmann (2000) described mud-rich debris flow deposits associated with mass-transport complexes and sand-prone high concentration turbidites associated with distributary channel-lobe complexes. The sand-rich sediment gravity flows occurred and increased in relative importance during the most recent sea level regression that began 115 to 125 thousand years ago (ka) and culminated at 15 ka (Mallarino *et al*., 2006). The constrained timing of concentrated sedimentation in the Brazos-Trinity Basin IV appears to be just slightly younger than that predicted from local biostratigraphic markers in the Diana basin and from seismic correlation between the two basins.

Gas Source and Migration

The two primary target areas in the Diana basin (Site EB 992 and Site AC 21) have at least three common elements that indicate that gas has been delivered to the gas hydrate stability zone. First, both are located over known deeper accumulations of conventional oil and gas. The AC 21 Site sits vertically above the South Diana field (AC 65), which produces from reservoirs that are ~5850 fbsf. The EB 992 Site sits vertically over the Rockefeller field (EB 992), where completion depths are expected to be ~4800 to 4950 fbsf. The Rockefeller reservoir is Lower Pleistocene (~1.7 my) in age (Symington and Higgins, 2000), and believed to be the stratigraphically youngest interval in the basin where conventional hydrocarbons have been found. Second, both of the sites are located over or near areas of broad positive relief as mapped by the authors at the top of the Lower Pleistocene (~0.8 my) and on the Regional 1 horizon (<0.44 my). At the AC 21 Site, this includes both the steep north-

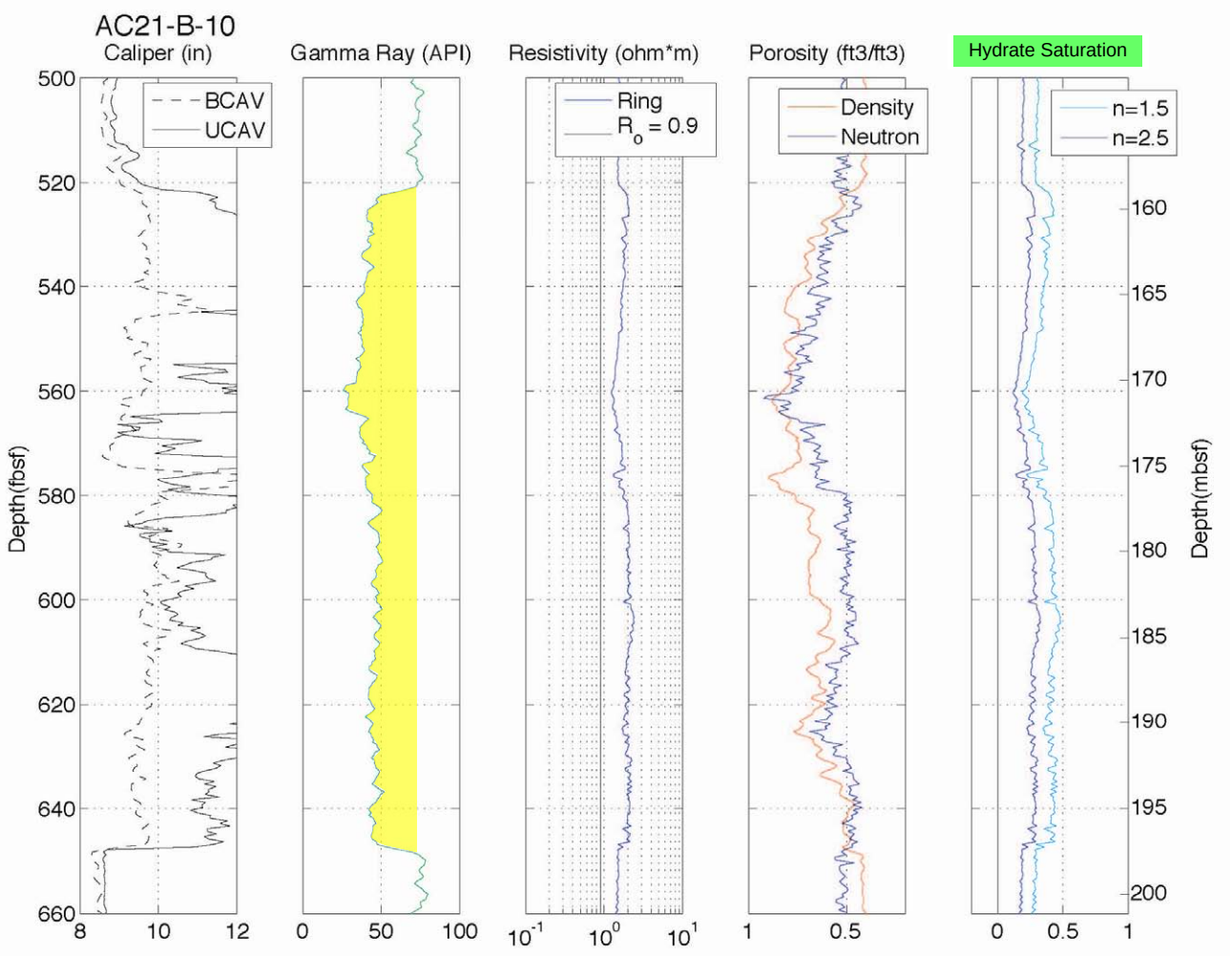

Figure F20: *Calculated gas hydrate saturation, AC 21-B well using Archie's quick-look method for two assumed values for exponent n (Guerin et al., 2009).*

dipping structural relief in blocks AC 65 and AC 66 generated by shallow salt emplacement to the south, as well as a series of closed structural highs that trend through blocks AC 21 and 22. Seismic amplitude anomalies extracted at the Lower Pleistocene level in some cases coincide with the structural features, and are believed to be gas-charged sediment. A similar WSW/ENE anticlinal ridge is well-developed south of and through the EB 992 Site. Evidence of fluid migration above and seismic data wipeout from gas below these structural features is highlighted in Figure F21. Third, both of our target Sites can be linked to at least one fault that cuts the Regional 1 horizon and continues with depth. The Regional 1 horizon is displaced by SW/NE trending, down to the NW normal faults. These fault systems align with depth to the positive structural features of Regional 1 and Lower Pleistocene horizons, as described above, and likely provide a linked system of gas migration first into the deep positive structural features and then into the shallow section via fault conduits.

At the EB 992 Site, it can be shown that the fault (hereafter the "Rockefeller fault") displaces the gas hydrate target sand facies, with minimal throw (< 100 ft), less than one half mile east of the proposed JIP target EB 992-C location. The offset is limited such that the gas hydrate target sand remains in communication across the fault. The Rockefeller fault propagates down section and intersects the Rockefeller reservoir at depth. Symington and Higgins (2000) found that the gas in the Rockefeller field reservoir is of biogenic origin, and concluded that the migration pathways for thermogenic hydrocarbons (typically sourced from lower Tertiary to Cretaceous rocks) into the prospect were inadequate. From this we conclude that the charge to Site EB 992 is likely partially biogenic in origin, derived from both focused flow along the Rockefeller fault and from near *in situ* conversion of organic carbon to methane by microbial processes.

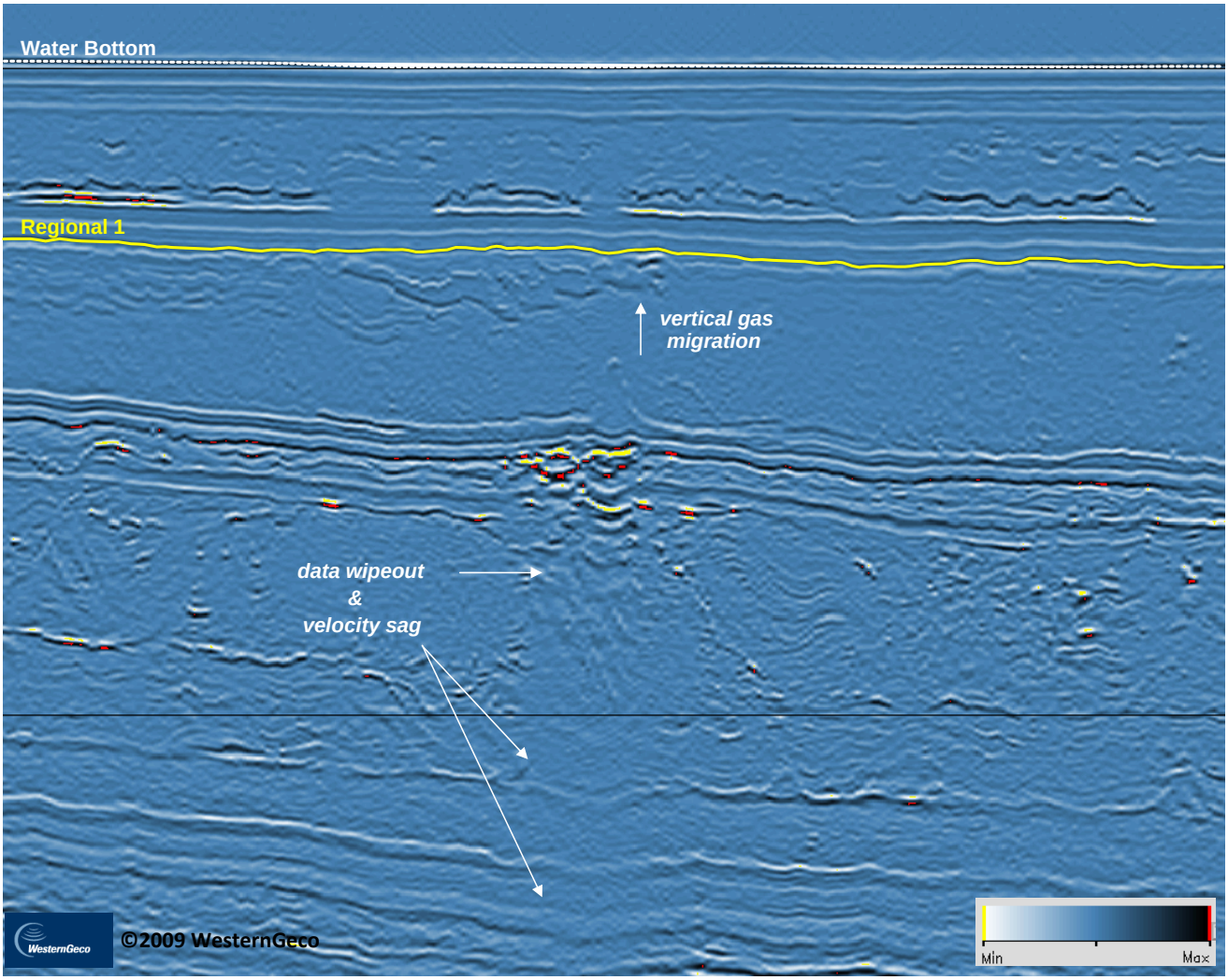

Figure F21: *Arbitrary seismic section through Site AC 21 showing focused vertical gas migration from depth. Seismic data courtesy of WesternGeco.*

The primary through-going fault that cuts the AC 21 target facies does so at least 1.5 miles east the JIP AC 21-B well. The argument can be made that gas entering our target reservoir through this fault would migrate in the general up-dip direction to the southeast, thus charging our reservoir facies and providing the amplitude response seen over the AC 21 site. Additionally, although not directly observed on seismic data, one can surmise that the South Diana fault, identified by Symington and Higgins (2000) as a viable migration pathway for thermogenic hydrocarbons into the South Diana field, could also contribute charge to the gas hydrate target facies. Conditions at the AC 21 Site are also believed to be favorable for *in situ* or near *in situ* conversion of organic carbon to methane by microbial processes.

Thus far we have presented evidence showing a strong likelihood for the presence of gas hydrate occurrence in the target sand intervals at low to moderate concentrations (20% to 40% S_{gh}) based on analysis of the LWD data and an understanding of the charge and migration processes at work in the Diana basin. In suggesting the presence of low to moderate S_{gh}, we are implicitly stating that the shallow section and highly porous reservoir sands are moderately-charged to under-charged. The possibility remains, however, that other factors could yield the anomalous resistivity log responses we interpret to indicate gas hydrate, including reservoir mineralogy, thin bed effects, and formation water salinity, whereby the sand reservoirs have not received any gas charge at all. Even after Leg II data acquisition and initial evaluation, the question still remains for either case: why is the shallow section not fully charged?

Of the many possibilities, the most likely explanation is that the age of the target reservoir is very young. If the charge is assumed to be thermogenic (gas composition is unknown

at this time), then the absolute age of the reservoir could affect the S_{gh} in two ways. First, the reservoir may be much younger than the time of maturation and expulsion of thermal hydrocarbons, and may have missed charging opportunities entirely. Second, the very young reservoir could actually be in the process of charging, the duration of which has not been sufficient for full methane saturation. This second argument would also apply to an assumed *in situ* biogenic gas source, whereby the sands simply have not been in place long enough to receive a fully saturated charge.

The complexity of the petroleum system and the notion of disparate or partial charge is further highlighted by the presence of the genetically related water-saturated sands (R_w = 0.2 Ω-m) in the EB 990 #001 well, which is ~4.1 miles NE of the AC 21-B location. The close proximity of these sands in a water-wet, rather than partially-charged, state would seem to suggest that local variations in pore water salinity or mineralogical composition are not likely. The one significant difference between the wet sands at the EB 990 well, the potentially gas hydrate-saturated sands at the EB 992 #001, the AC 21-A, and the AC 21-B wells is that the charged sands in the latter three wells are vertically-isolated bodies that are more deeply-buried (although yet still very shallow) and therefore with greater potential for top seal integrity, whereas the EB 990 #001 well sands are stacked to a gross thickness of at least 550 ft with no apparent top seal.

Conclusions

The primary goal of the Gulf of Mexico JIP Leg II drilling program was to locate and record the occurrence of gas hydrate in high-quality deepwater sand reservoirs. In the first week of May 2009, the JIP utilized the Helix Q-4000 semi-submersible to drill and log two wells in the Diana sub-basin in the western Gulf of Mexico at the Alaminos Canyon 21 Site. The AC 21-A and AC 21-B wells confirmed the presence of an areally extensive, sand-rich deepwater fan system that was predicted from industry 3-D seismic data and existing industry well penetrations. The primary targets were encountered within 600 ft of the seafloor, well above the predicted base of gas hydrate stability depth of approximately 1500 fbsf. The target sand reservoirs as seen in the A and B wells measured 62 ft and 125 ft, respectively, and contained elevated formation resistivity consistent with low to moderate saturations of gas hydrate (20% to 40%). The interface between the overlying shales and the hydrate-bearing sands is one of high acoustic impedance, thus providing an anomalous response on the 3-D seismic data with a strong peak-leading top.

Acknowledgements

The authors would like to acknowledge contributions from the following: the JIP site selection team, the Leg II onboard science party, and the captain and crew of the Helix *Q-4000* drilling vessel. Proprietary seismic data was provided by Western Geco.

References

Beaubouef, R. T., and S. J. Friedmann, 2000. High resolution seismic/sequence stratigraphic framework for the evolution of the Pleistocene intra slope basins, western Gulf of Mexico: Depositional models and reservoir analogs, *in* P. Weimer, R. M. Slatt, J. Coleman, N. C. Rosen, H. Nelson, A. H. Bouma, M. J. Styzen, and D. T. Lawrence, eds., Deep-water reservoirs of the world: Proceedings of the 20th Annual Research Conference, Gulf Coast Section SEPM Foundation, p. 40–60.

Beaubouef, R. T., V. Abreu, J. C. Van Wagoner, 2003. Basin 4 of the Brazos-Trinity slope system, western Gulf of Mexico: The terminal portion of a late Pleistocene lowstand system tract, *in* H. H. Roberts, N. C. Rosen, R. H. Fillon, and J. B. Anderson, eds., Shelf margin deltas and linked down slope petroleum systems: Global significance and future exploration potential: Proceedings of the 23rd Annual Research Conference, Gulf Coast Section SEPM Foundation, p. 45– 66.

Boswell, R., Hutchinson, D., and Ray, P., 2005. Changing perspectives on the resource Potential of Methane Hydrates, DOE-NETL Fire in the Ice Newsletter, Summer, p. 1-5.

Boswell, R., Collett, T.S., Frye, M., McConnell, D., Shedd, W., Mrozewski, S., Guerin, G., and Cook, A., 2009a. Gulf of Mexico Gas Hydrate Joint Industry Project Leg II — Technical Summary: Proceedings of the Drilling and Scientific Results of the 2009 Gulf of Mexico Gas Hydrate Joint Industry Project Leg II. http://www.netl.doe.gov/technologies/oil-gas/publications/Hydrates/2009Reports/TechSum.pdf

Boswell, R., D. Shelander, M. Lee, T. Latham, T. Collett, G. Guerin, G. Moridis, M. Reagan, and D. Goldberg, 2009b. Occurrence of gas hydrate in Oligocene Frio sand: Alaminos Canyon Block 818: Northern Gulf of Mexico, Marine and Petroleum Geology (2009), doi:10.1016/j.marpetgeo.2009.03.005.

Bruno, R.S., and Hanor, J.S., 2003. Large-scale fluid migration driven by salt dissolution, Bay Marchand dome, offshore Louisiana: Gulf Coast of Geological Societies Transactions, v. 53, p. 97-107.

Collett, T.S., Johnson, A., Knapp, C., Boswell, R., 2009a. Natural Gas Hydrates – A Review: in Collett, T., *et al*., eds, *Natural Gas Hydrates: Energy Resource and Associated Geologic Hazards*; American Association of Petroleum Geologists Memoir 89.

Collett, T.S., Boswell, R., Mrozewski, S., Guerin, G., Cook, A., Frye, M., Shedd, W., and McConnell, D., 2009. Gulf of Mexico Gas Hydrate Joint Industry Project Leg II — Operational Summary: Proceedings of the Drilling and Scientific Results of the 2009 Gulf of Mexico Gas Hydrate Joint Industry Project Leg II. http://www.netl.doe.gov/technologies/oil-gas/publications/Hydrates/2009Reports/OpSum.pdf

Collett, T.S., Riedel, M., Cochran, J., Boswell, R., Presley, J., Kumar, P., Sathe, A., Sethi, A., Lall, M., Siball, V., and the NGHP Expedition 01 Scientific Party, 2008. Indian National Gas Hydrate Program Expedition 01 Initial Reports: Prepared by the U.S. Geological Survey and Published by the Directorate General of Hydrocarbons, Ministry of Petroleum & Natural Gas (India), 1 DVD.

Collett, T.S., 2000. Quantitative well-log analysis of in-situ natural gas hydrate: Ph.D. Thesis, Colorado School of Mines, Golden, Colorado, 535 p.

Collett, T.S., 1998. Well log evaluation of gas hydrate saturations: Transactions of the Society of Professional Well Log Analysts, Thirty-Ninth Annual Logging Symposium, paper MM.

Dai, J., H. Xu, F. Snyder, and N. Dutta, 2004. Detection and estimation of gas hydrates using rock physics and seismic inverstion: Examples from the northern deepwater Gulf of Mexico, The Leading Edge, January, p. 60-66.

Flemings, P.B., Behrmann, J.H., John, C.M., and the Expedition 308 Scientists, 2006. Proc. IODP, 308: College Station TX (Integrated Ocean Drilling Program Management International, Inc.). doi:10.2204/iodp.proc.308.2006

Frye, M., 2008, Preliminary Evaluation of In-Place Gas Hydrate Resources: Gulf of Mexico Outer Continental Shelf, OCS Report MMS 2008-004, 94 pages.

Gradstein, F.M., Ogg, J.G., and Smith, A.G., 2004. A Geologic Time Scale 2004, Cambridge University Press, Cambridge.

Gregory, A.R., 1977. Aspect of rock physics form laboratory and log data that are important to seismic interpretation, in Payton, C.E. ed., Seismic stratigraphy— applications to hydrocarbon exploration, AAPF Memoir 26, p.15-46.

Guerin, G., Cook, A., Mrozewski, S., Collett, T.S., Boswell, R., 2009. Gulf of Mexico Gas Hydrate Joint Industry Project Leg II — Alaminos Canyon 21 LWD Operations and Results: Proceedings of the Drilling and Scientific Results of the 2009 Gulf of Mexico Gas Hydrate Joint Industry Project Leg II. http://www.netl.doe.gov/technologies/oil-gas/publications/Hydrates/2009Reports/AC21LWDOps.pdf

Hadley, C., Peters, D., Vaughan, A., and Bean, D., 2008. Gumusut-Kakap Project: Geohazard characterization and impact on field development plans, International Petroleum Technology Conference paper 12554, IPTC conference in Kuala Lumpur, Malaysia, 3-5 December, 2008.

Hanor, J.S., 2007. Pre-production spatial variation in formation water salinity in a deepwater Gulf of Mexico field, *in* Bullen, T., and Wang, Y., eds., Water-Rock Interaction, Taylor and Francis Group, London, p. 505-508.

Hanor, J.S., 2004. The role of salt dissolution in the geologic, hydrologic, and diagenetic evolution of the northern Gulf Coast sedimentary basin, in Post, P.J., ed., Salt-sediment interactions and hydrocarbon prospectivity: concepts and case studies for the 21st century, 24th Annual Gulf Coast Section SEPM Foundation Research Conference, p. 464-501.

Harris, R.N., Fisher, A.T., Martinez, F., and Ruppel, C., 2007. Workshop on The Future of Marine Heat Flow: Defining Scientific Goals and Experimental Needs for the 21st Century; 6-7 September 2007; Fort Douglas, University of Utah, UT.

Hood, K. C., L. M. Wenger, O. P. Gross, and S. C. Harrison, 2002. Hydrocarbon systems analysis of the northern Gulf of Mexico: Delineation of hydrocarbon migration pathways using seeps and seismic imaging, in Surface exploration case histories: Applications of geochemistry, magnetics, and remote sensing, D. Schumacher and L. A. LeSchack, eds., AAPG Studies in Geology No. 48 and SEG Geophysical References Series No. 11, p. 25–40.

Hutchinson, D., Boswell, R., Collett, T.S., Dai, J., Dugan, B., Frye, M., Jones, E., McConnell, D., Rose, K., Ruppel, C., Shedd, W., Shelander, D., Wood, W., 2009a. Gulf of Mexico Gas Hydrate Joint Industry Project Leg II — Walker Ridge 313 Site Selection: Proceedings of the Drilling and Scientific Results of the 2009 Gulf of Mexico Gas Hydrate Joint Industry Project Leg II. http://www.netl.doe.gov/technologies/oil-gas/publications/Hydrates/2009Reports/WR313SiteSelect.pdf

Hutchinson, D., Boswell, R., Collett, T.S., Dai, J., Dugan, B., Frye, M., Jones, E., McConnell, D., Rose, K., Ruppel, C., Shedd, W., Shelander, D., Wood, W., 2009b. Gulf of Mexico Gas Hydrate Joint Industry Project Leg II — Green Canyon 955 Site Selection: Proceedings of the Drilling and Scientific Results of the 2009 Gulf of Mexico Gas Hydrate Joint Industry Project Leg II. http://www.netl.doe.gov/technologies/oil-gas/publications/Hydrates/2009Reports/GC955SiteSelect.pdf

Inks, T., Lee, M., Agena, W., Taylor, D., Collett, T., Hunter, R., and Zyrianova, M., 2009. Prospecting for gas hydrate accumulations using 2-D and 3-D seismic data, Milne Point, North Slope, Alaska, in Collett, T.S., Johnson, Art, Knapp, Camelia, and Boswell, Ray, eds., Natural Gas Hydrates —– Energy Resource Potential and Associated Geologic Hazards: AAPG Memoir 89, p 1-29.

Lee, M. W. and T. S. Collett, 2009. Gas hydrate saturations estimated from fractured reservoir at Site NGHP-01-10, Krishna-Godavari Basin, India, J. Geophys. Res.114.10.1029/2008jb006237

Lorenson, T.D., and Collett, T.S., 2000. Gas content and composition of gas hydrate from sediments of the southeastern North American continental margin, in Paull, C.K., Matsumoto, R., Wallace, P.J., and Dillon, W.P. (Eds.), 2000. Proc. ODP, Sci. Results, 164: College Station, TX (Ocean Drilling Program).

Mallarino, G., Beaubouef, R.T., Droxler, A.W., Abreu, V., and Labeyrie, L., 2006. Sea level influence on the nature and timing of a minibasin sedimentary fill (northwestern slope of the Gulf of Mexico), AAPG Bulletin, v. 90, no. 7 (July 2006), pp. 1089–1119.

Marcucci, E., and J. Forrest, 2007. Potential extent and thickness of gas hydrates in the deep water of the northern Gulf of Mexico: Gulf Coast Association of Geological Societies Transactions, v. 57, p. 557-568.

McConnell, D., Boswell, R., Collett, T.S., Frye, M., Shedd, Wi., Guerin, G., Cook, A., Mrozewski, S., Dufrene, R., Godfriaux, P., 2009. Gulf of Mexico Gas Hydrate Joint Industry Project Leg II — Green Canyon 955 Site Summary: Proceedings of the Drilling and Scientific Results of the 2009 Gulf of Mexico Gas Hydrate Joint Industry Project Leg II. http://www.netl.doe.gov/technologies/oil-gas/publications/Hydrates/2009Reports/GC955SiteSum.pdf

Milkov, A.V., and Sassen, R., 2001. Estimate of gas hydrate resource, northwestern Gulf of Mexico continental slope, Marine Geology, vol. 179, p 71-83.

Mrozewski, S., Guerin, G., Cook, A., Collett, T.S., Boswell, R., 2009. Gulf of Mexico Gas Hydrate Joint Industry Project Leg II — LWD Methods: Proceedings of the Drilling and Scientific Results of the 2009 Gulf of Mexico Gas Hydrate Joint Industry Project Leg II. http://www.netl.doe.gov/technologies/oil-gas/publications/Hydrates/2009Reports/LWDMethods.pdf

O'Brien, J.J., and Lerche, I., 1988, Impact of heat flow anomalies around salt sheets in the Gulf Coast on hydrocarbon maturity: model and observations: Transactions of the Gulf Coast Association of Geological Societies, vol. 38, p. 213-245.

Shedd, W., Frye, M., Boswell, R., Hutchinson, D., and Godfriaux, P., 2009a. Variety of seismic expression of the base of gas hydrate stability in the Gulf of Mexico, USA, AAPG Annual Convention and Exhibition Abstracts, Denver, Colorado, June 7-10, 2009.

Shedd, W., Hutchinson, D., Boswell, R., Collett, T.S., Dai, J.C., Dugan, B., Frye, M., Jones, E., McConnell, D., Rose, K., Ruppel, C., Shelander, D., and Wood, W., 2009b. Gulf of Mexico Gas Hydrate Joint Industry Project Leg II — East Breaks 991 and Alaminos Canyon 21 Site Selection: Proceedings of the Drilling and Scientific Results of the 2009 Gulf of Mexico Gas Hydrate Joint Industry Project Leg II. http://www.netl.doe.gov/technologies/oil-gas/publications/Hydrates/2009Reports/AC21SiteSelect.pdf

Sullivan, M.D., J.L. Foreman, D.C. Jennette, D. Stern, G.N. Jensen, and F.J. Goulding, 2004, An integrated approach to characterization and modeling of deep-water reservoirs, Diana field, western Gulf of Mexico, in Integration of outcrop and modern analogs in reservoir modeling: AAPG Memoir 80, p. 215-234.

Sullivan, M., and P. Templet, 2002. Characterization of fine-grained deep-water turbidite reservoirs: Examples from Diana Sub-Basin western Gulf of Mexico, GCSSEPM Foundation Deep-Water Core Workshop, Northern Gulf of Mexico, Houston, TX, p. 75-92.

Symington, W. A., and J. W. Higgins, 2000. Migration pathway analysis contributes to success in the Diana Intraslope Basin, western Gulf of Mexico, Hedberg 1998 models for understanding risk, p. 1-9.

Waite, W.F., Santamarina, J.C., Cortes, D., Dugan, B., Espinoza, D.N., Germaine, J., Jang, J., Jung, J.W., Kneafsey, T.J., Shin, H., Soga, K., Winters, W.J., Yun, T.S., 2009. Physical properties of hydrate-bearing sediments. Reviews of Geophysics, vol. 47, RG4003, DOI:10.1029/2008RG000279

Western Geco, 2009. http://www.multiclient.westerngeco.com/NavPDFs%5CEB_AC8-Q.pdf.

Witrock, R. B., A. R. Friedmann, J. J. Galluzzo, L. D. Nixon, P. J. Post, and K. M. Ross, 2003. Biostratigraphic chart of the Gulf of Mexico offshore region, Jurassic to Quaternary, U. S. Department of the Interior, Minerals Management Service, New Orleans.

Yamano, M., Uyeda, S., Aoki, Y., and Shipley, T. H., 1982. Estimates of heat flow derived from gas hydrates: Geology, v. 10, p. 339–343.